Water Resources Research

RESEARCH ARTICLE
10.1029/2023WR034786

A Multivariate Frequency Analysis Framework to Estimate the Return Period of Hurricane Events Using Event-Based Copula

Eunsaem Cho[1,2], Ebrahim Ahmadisharaf[1,2], James Done[3], and Chulsang Yoo[4]

[1]Department of Civil and Environmental Engineering, FAMU-FSU College of Engineering, Florida State University, Tallahassee, FL, USA, [2]Resilient Infrastructure and Disaster Response Center, FAMU-FSU College of Engineering, Florida State University, Tallahassee, FL, USA, [3]National Center for Atmospheric Research, Boulder, CO, USA, [4]School of Civil, Environmental and Architectural Engineering, College of Engineering, Korea University, Seoul, Korea

Key Points:

- We introduced a new framework for evaluating multivariate return periods of hurricane events through event-based frequency analyses
- Using this framework, we estimated the univariate, bivariate, and trivariate return periods of Hurricane Ian
- A return period map was produced using the framework to identify the HUC8 basins affected by Hurricane Ian

Supporting Information:

Supporting Information may be found in the online version of this article.

Correspondence to:

E. Ahmadisharaf,
eahmadisharaf@eng.famu.fsu.edu;
eascesharif@gmail.com

Citation:

Cho, E., Ahmadisharaf, E., Done, J., & Yoo, C. (2023). A multivariate frequency analysis framework to estimate the return period of hurricane events using event-based copula. *Water Resources Research*, *59*, e2023WR034786. https://doi.org/10.1029/2023WR034786

Received 3 MAR 2023
Accepted 31 OCT 2023

Author Contributions:

Conceptualization: Ebrahim Ahmadisharaf
Methodology: Ebrahim Ahmadisharaf, James Done, Chulsang Yoo
Supervision: Ebrahim Ahmadisharaf
Writing – review & editing: Ebrahim Ahmadisharaf, James Done, Chulsang Yoo

Abstract This study proposed a framework to evaluate multivariate return periods of hurricanes using event-based frequency analysis techniques. The applicability of the proposed framework was demonstrated using point-based and spatial analyses on a recent catastrophic event, Hurricane Ian. Univariate, bivariate, and trivariate frequency analyses were performed by applying generalized extreme value distribution and copula on annual maximum series of flood volume, peak discharge, total rainfall depth, maximum wind speed, wave height and storm surge. As a result of point-based analyses, return periods of Hurricane Ian was investigated by using our framework; univariate return periods were estimated from 39.2 to 60.2 years, bivariate from 824.1 to 1,592.6 years, and trivariate from 332.1 to 1,722.9 years for the Daytona-St. Augustine Basin. In the Florida Bay-Florida Keys Basin, univariate return periods were calculated from 7.5 to 32.9 years, bivariate from 36.5 to 114.9 years, and trivariate from 25.0 to 214.8 years. Using the spatial analyses, we were able to generate the return period map of Hurricane Ian across Florida. Based on bivariate frequency analyses, 18% of hydrologic unit code 8 (HUC8) basins had an average return period of more than 30 years. Sources of uncertainty, due to the scarcity of analysis data, stationarity assumption and impact of other weather systems such as strong frontal passages, were also discussed. Despite these limitations, our framework and results will be valuable in disaster response and recovery.

1. Introduction

Tropical cyclones (TCs) can lead to significant economic damages and death tolls across TC-prone global regions (Rappaport, 2014). The normalized cost of hurricane damage in the United States is estimated to be $1.9 trillion from 1900 to 2017, with a normalized annual average of $16.7 billion (Weinkle et al., 2018). Between 1980 and 2022, hurricane-related fatalities totaled 6,751 across the United States (NCEI, 2023). One of the most devastating hurricanes in the United States was Hurricane Katrina in 2005, which resulted in ~$186 billion in damages (in 2022 dollars) and 1,392 deaths (Knabb et al., 2023). In 2022, Hurricane Ian caused substantial damage to the United States, which resulted in 156 fatalities and losses estimated at $112.9 billion (NCEI, 2023; NHC, 2022). These huge losses in the past may become even more substantial in the future due to climate change and changes in exposure and vulnerability as a result of population growth, aging infrastructure, and land development (Dinan, 2017; Estrada et al., 2015; Pant & Cha, 2019).

Many researchers have provided evidence for stronger TCs due to climate change (Camelo et al., 2020; Emanuel, 2011; Gori et al., 2022; Holland & Bruyère, 2014; Hosseini et al., 2018; Li et al., 2023; Ting et al., 2019), with stronger TCs already detected in the recent historical record (Kossin et al., 2020). There has been an increase in the proportion of North Atlantic TCs that become major hurricanes and the proportion of TCs that intensify rapidly (Balaguru et al., 2018; Bhatia et al., 2019; Song, Alipour, et al., 2020; Song, Duan, & Klotzbach, 2020; Vecchi et al., 2021). At the same time, a signal of climate change has been detected in increased TC rainfall rates in some regions (e.g., Emanuel, 2017). These trends are expected to continue in the future (Knutson et al., 2020) with increased peak wind speeds combining with higher peak rainfall rates and higher storm surge due to sea level rise raising the multi-hazard threat to coastal regions (Lin et al., 2012; Marsooli et al., 2019; Mayo & Lin, 2022).

A key component to understanding the risk of hurricane-related damages is the estimation of a realistic frequency for hurricane events. To address this, the concept of exceedance probability (the inverse commonly referred to as the return period) has been widely adopted. Engineered structures such as hydraulic structures and pipe networks are designed based on the return period. During the past two decades, many studies explored frequency analyses

of meteorologic and hydrologic data (Chebana & Ouarda, 2011; Favre et al., 2004; Genest et al., 2007; Laio et al., 2009; Li et al., 2019, 2023; Salvadori & De Michele, 2004; Yue & Rasmussen, 2002; Q. Zhang et al., 2014; L. Zhang & Singh, 2006). Hurricane-related frequency analyses began with direct analyses of historical records (Elsner & Kara, 1997; Keim et al., 2007). Since then, various meteorologic and hydrologic data, such as wind speed, precipitation, flow discharge, and storm surge, have been statistically analyzed to estimate the return periods of the multiple hazards posed by hurricanes.

Univariate frequency analyses of hurricanes have been mostly based on wind speed and precipitation (Elsner et al., 2006; Emanuel, 2017; Emanuel & Jagger, 2010; Keellings & Hernández Ayala, 2019; Regier et al., 2022; Van Oldenborgh et al., 2017; Vu & Mishra, 2019). For example, Elsner et al. (2006) evaluated the return period of Hurricane Katrina by examining the maximum wind speeds that affected the United States from 1899 to 2004, and used the generalized Pareto distribution to perform the frequency analyses. Van Oldenborgh et al. (2017) calculated the return period of Hurricane Harvey's rainfall by applying the generalized extreme value (GEV) distribution to the annual maximum 3-day rainfall data in Houston, Texas. Peak discharge has also been considered as a major variable in univariate analyses. For Hurricane Harvey's flood return period estimations, McDonald and Naughton (2019) applied the Log Pearson III distribution and Nyaupane et al. (2018) applied the GEV to discharge data. However, these univariate assessments miss potentially important dependencies between hazards and misrepresent the likelihood of high-impact conditions (Harr et al., 2022).

In bivariate and trivariate probability estimates, copula theory is commonly used to interpret precipitation, wind speed, flow discharge, and storm surge data (Alipour et al., 2022; Harr et al., 2022; Latif & Simonovic, 2022; Meng et al., 2021; Phillips et al., 2022; Sebastian et al., 2017; Trepanier et al., 2015; Wahl et al., 2015; B. Zhang et al., 2022). For example, Trepanier et al. (2015) examined the correlation and joint exceedance probability of wind speed and storm surge in Galveston, Texas, during the period of 1900–2008. Sebastian et al. (2017) examined the Gulf of Mexico hurricane probabilities using copula and hourly storm surge and daily precipitation data from 1900 to 2014. Harr et al. (2022) explored joint probabilities of TC rainfall and wind speeds. Phillips et al. (2022) applied copula to tide level and rainfall data in Florida, Georgia, and South Carolina, and analyzed the frequency of Hurricane Irma, which occurred in 2017. For trivariate frequency analyses, Latif and Simonovic (2022) examined rainfall, flow discharge, and sea level data in Vancouver, Canada, and established a relationship among the existing univariate, bivariate, and trivariate frequency analysis results.

While several studies have focused on TC rainfall, wind speed, and storm surge, comprehensive investigations into these characteristics and their dependencies using state-of-the-art analysis techniques have been limited (Latif & Simonovic, 2022; Ming et al., 2022). Additionally, it is challenging to find comprehensive examinations of spatial characteristics of multivariate hurricane frequency. Since most studies examined data from limited numbers of point locations or area-averaged data, it is difficult to assess the spatial distribution of hurricane frequency. Another limitation in the body of literature is that previous studies used point times of observations rather than defining events over the actual duration of hurricanes. The term “point times of observation” refers to specific moments when data is collected, whereas the “actual duration of hurricanes” denotes the complete time span in which the hurricane events occur. Due to the fact that a hurricane may not perfectly match the time of observation, the uncertainty of frequency analyses can be rather high. This is a major source of uncertainty identified by frequency analysis studies of rainfall events (Jun et al., 2018; Kao & Govindaraju, 2007; Lee et al., 2010; Yoo & Cho, 2019).

The objective of this study is to develop a framework for event-based analyses of hurricanes using three frequency analysis techniques: univariate, bivariate, and trivariate. We demonstrate this framework on Hurricane Ian, a catastrophic hurricane in September 2022 that affected a large swath of the Southeastern United States. This study also examines the spatial distribution of hurricane frequency through univariate and bivariate frequency analyses of data from over 70 weather stations (for wind speed and rainfall), stream gauges (for flow discharges) and tidal gauges (for sea levels) in Florida. The novelty of this study lies in three key aspects. First, it introduces event-based frequency analyses as a more realistic approach for assessing hurricane risks, which is known to be more realistic than relying on the duration of observed rainfall events (Adams & Papa, 2001; Balistrocchi & Bacchi, 2011; Jun et al., 2018; Yoo et al., 2016). Second, by encompassing a broader range of variables, including rainfall, wind speed, flow discharge, and sea level, this paper offers a framework for comprehensive assessments of hurricane risks. Lastly, the framework expands upon existing methodologies by incorporating various frequency analysis techniques (univariate, bivariate, and trivariate) consistently applied at an hourly time scale.

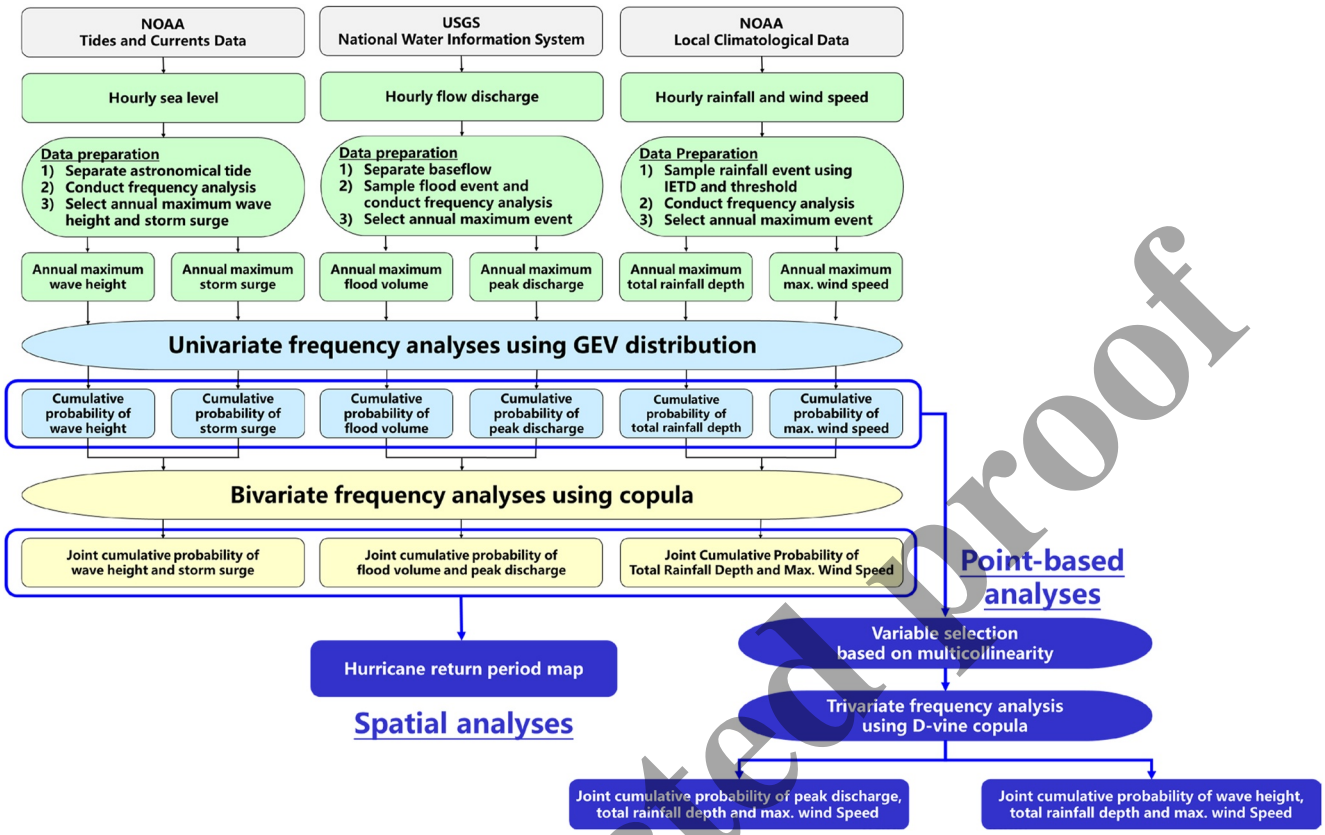

Figure 1. Schematic of the framework for point-based and spatial analyses. GEV: Generalized Extreme Value.

These innovative aspects allow for a deeper understanding of hurricane risks and provide more detailed insights into their effects.

2. Methodology

2.1. Framework for Hurricane Frequency Analyses

This study presents a framework to conduct two types of frequency analyses: (a) point-based; and (b) spatial. For the point-based analyses, we apply univariate, bivariate and trivariate analyses on a single site to estimate return periods. For the spatial analyses, we perform univariate and bivariate analyses on multiple sites to investigate the spatial distribution of hurricane frequency. Trivariate analyses are not performed for the spatial analysis due to lack of data on all required variables across the geographic domain, but the framework accommodates trivariate spatial analyses if the data are available. Figure 1 illustrates a schematic of the framework for point-based and spatial analyses. The application of the framework present here is for flow discharge, rainfall, wind, and sea level, but the framework is flexible to other pertinent variables.

To apply the event-based analyses, we use historical hourly data for flow discharge, rainfall, wind speed, and sea level. Annual maximum series of flood volume, peak discharge, total rainfall depth, maximum wind speed, wave height, and storm surge were prepared for the frequency analyses. Univariate frequency analyses are conducted using GEV distribution, the common choice in analyses using annual maxima approach (Alaya et al., 2020; Engeland et al., 2004; Faranda et al., 2011; Katz et al., 2002), and bivariate frequency analyses are conducted via copula. Trivariate frequency analyses are conducted by applying D-vine copula to sites with weather stations and stream gauges that are in close proximity as determined by being within the same hydrologic unit code 8 (HUC8) basin. In all frequency analyses, 95% confidence intervals of return periods are derived based on estimated parameters of the GEV within those intervals.

In the process of evaluating the return period of Hurricane Ian, we excluded the observed data in 2022 for deriving the GEV distribution and copulas. The flood volume, peak discharge, total rainfall depth, maximum wind

speed, wave height, and storm surge of Hurricane Ian were then evaluated based on the derived GEV distribution and copula using all years, except for 2022. The events that occurred between September 23 and 30, 2022 (the hurricane period) were selected for evaluating Hurricane Ian. For example, an event already in progress at the time of the hurricane or an event that occurred during the occurrence period was selected as one of the representative events for Hurricane Ian.

2.2. Selection of Annual Maximum Series

The first step of the frequency analysis is to determine annual maximum series or partial duration series of target time series. This study uses block maxima approach to sample annual maximum series using multi-criteria decision analyses. The annual maximum series can be chosen through the block maxima approach. This approach selects the event that has the greatest value within a specific period (e.g., 1 year). In contrast to the block maxima approach, the peak-over-threshold method samples maximum series using a specific threshold, allowing for the inclusion of more extreme data points. Both approaches have been widely applied in previous frequency analysis research (Engeland et al., 2004; Lombardo et al., 2019; Prosdocimi et al., 2015).

The advantage of the block maxima approach is that it guarantees the independence of the selected events (Brunner et al., 2016; Ferreir and De Haan, 2015; Tabari, 2021). By applying the block maxima approach in flood frequency analyses, it is possible to consider annual peak floods as independent and identically distributed series (Yan & Moradkhani, 2015). In addition, the use of the block maxima approach is appropriate for applying multi-criteria on annual maximum series selection. Several studies selected annual maximum series based on multi-criteria decision analyses (Kao & Govindaraju, 2007; Park et al., 2014; Yoo & Cho, 2019; Yoo et al., 2016).

2.3. Theory of Copula

Copula is a mathematical method to derive a multivariate cumulative distribution function (CDF) based on various marginal CDFs (Favre et al., 2004; Genest & Favre, 2007; Nelsen, 2007; Salvadori & De Michele, 2004; Sklar, 1959). The advantage of copula is that any type of marginal CDFs can be used to derive multivariate CDFs (Dupuis, 2007; Salvadori & De Michele, 2007; L. Zhang & Singh, 2007). As a result, a copula-based multivariate CDF can represent characteristics of the applied marginal CDF. The fundamental equation explaining the copula can be expressed as Equation 1.

$$H(x_1, x_2, ..., x_n) = C[F_1(x_1), F_2(x_2), ..., F_n(x_n)] \quad (1)$$

where H is the cumulative probability, C is the copula, and $F_i(x_i)$ is cumulative probability that is calculated using the ith marginal CDF. Equation 1 shows that the copula can be used to combine n marginal CDFs into a single multivariate CDF.

Copulas can be categorized into three major families: Archimedean copulas, elliptical copulas, and Marshall-Olkin copulas (Embrechts et al., 2001). The Archimedean and elliptical copula family are selected for our analyses because copulas under these categories are relatively straightforward to construct and are well-known for their wide range of applications in frequency analyses of hydrologic problems (Nelsen, 2007). Of the existing copulas under the Archimedean family, we consider the Clayton (Clayton, 1978; Equation 2), the Frank (Frank, 1979; Equation 3), the Gumbel–Hougaard (Gumbel (1960); Equation 4), and the Joe (Joe, 1997; Equation 5) copulas. For the elliptical copula, we consider the Gaussian copula (Schmidt & Stadtmüller, 2006; Equation 6). Table 1 summarizes the bivariate CDFs of these copulas. In Table 1, θ is the parameter for copula, u_1 and u_2 are the cumulative probabilities calculated by the marginal CDF of each pair of two target variables. In the case of Φ, it is the inverse function of the standard normal distribution.

Parameter θ for each copula is estimated by applying maximum likelihood estimation method (MLE) (Ko & Hjort, 2019; Weiß, 2011; J. Zhang et al., 2022) and estimated values are evaluated whether they are in a valid range. The parameter θ for the Clayton copula must be defined in $[-1, \infty]$, except for zero, while the valid range for the Gumbel-Hougaard and Joe copula is $[1, \infty]$. The parameter θ for the Gaussian copula is valid within $[-1, 1]$, and Frank copula can be applied with any value of θ, except for zero.

Among these five copulas, this study selects one for the frequency analyses based on the Akaike information criterion (AIC; Akaike, 1974) and the Bayesian information criterion (BIC; Stone, 1979). These two criteria

Table 1
Joint Cumulative Distribution Function (CDF) of Copula Models Considered in This Study

Copula	Bivariate CDF	Equation
Clayton	$C(u_1,u_2)=\left(u_1^{-\theta}+u_2^{-\theta}-1\right)^{-1/\theta}$	(2)
Frank	$C(u_1,u_2)=-\frac{1}{\theta}\ln\left[1+\frac{(\exp(-\theta u_1)-1)(\exp(-\theta u_2)-1)}{\exp(-\theta)-1}\right]$	(3)
Gumbel–Hougaard	$C(u_1,u_2)=\exp\left(-\left((-\ln(u_1))^{\theta}+(-\ln(u_2))^{\theta}\right)^{1/\theta}\right)$	(4)
Joe	$C(u_1,u_2)=1-\left((1-u_1)^{\theta}+(1-u_2)^{\theta}-(1-u_1)(1-u_2)^{\theta}\right)^{1/\theta}$	(5)
Gaussian	$C(u_1,u_2)=\int_{-\infty}^{\Phi^{-1}(u_1)}\int_{-\infty}^{\Phi^{-1}(u_2)}\frac{1}{2\pi\sqrt{1-\theta^2}}\exp\left(-\frac{s^2+w^2-2sw\theta}{2(1-\theta^2)}\right)dsdw$	(6)

measure goodness-of-fit by maximum likelihood functions and penalize complexity by the number of parameters. The lower the AIC or BIC value, the better the fit.

This study uses *R* statistical package "stats" to calculate the maximum likelihood. The package utilizes the copula-based cumulative probability and empirical CDF as the inputs. The empirical cumulative probability of the given data was calculated here by computing their pseudo-observation, which is the normalized rank value.

The optimal copula determined by the lowest AIC and BIC is additionally tested with the Kolmogorov–Smirnov (K-S) statistic (Massey Jr, 1951). The K-S statistic is equal to the maximum absolute difference between the cumulative probability from copula and that from empirical equation. If the calculated K-S statistic is smaller than the critical value of the K-S test, the goodness-of-fit of the copula is guaranteed. For the critical value of the K-S test, the significance level is set to 5%. The critical value is calculated as 0.2242 for 35 years of records, and 0.2417 for 30 years of records.

2.4. Return Period Calculations

We use three frequency analysis methods—univariate, bivariate, and trivariate—to estimate the return period of a given hurricane event. The return period is the reciprocal of the exceedance probability. However, the method to calculate the exceedance probability depends on the method of frequency analysis.

2.4.1. Univariate Return Period

The simplest method to calculate the exceedance probability is that of univariate frequency analysis. In this method, the exceedance probability can be obtained by calculating the upper area of target value in probability density function (PDF). Since the return period is the reciprocal of the exceedance probability, the univariate return period T_{uni} can be expressed as Equation 7.

$$T_{\text{uni}}=\frac{1}{1-\Pr(X<x)}=\frac{1}{1-F_X(x)} \tag{7}$$

We use GEV distribution as the marginal PDF based on extreme value theory (Coles et al., 2001). For each variable, MLE method (White, 1982) is applied for parameter estimation and K-S test for goodness-of-fit test. MLE method and K-S test are conducted with R package "fitdistrplus" (Delignette-Muller & Dutang, 2015).

Annual maximum series of flood volume, peak discharge, total rainfall depth, maximum wind speed, wave height, and storm surge are used for univariate frequency analyses. The univariate return periods are calculated for each variable and compared with each other. In addition, cumulative probability of these variables is used as the input variable in the bivariate and trivariate frequency analyses.

2.4.2. Bivariate Return Period

This study calculates the bivariate return period based on the AND concept suggested by Yue and Rasmussen (2002) and Shiau (2003). Some studies have concluded that the AND return period is more reliable when it comes to modeling extreme events (Goel et al., 2000; Kurothe et al., 1997; Poulin et al., 2007), such as hurricanes that are our focus here. In the case of AND concept, the exceedance probability is calculated with the probability that both variables exceed target values. AND concept of return period T_{bi} is defined by Equation 8.

$$T_{bi} = \frac{1}{1 - F_X(x) - F_Y(y) + C(F_X(x), F_Y(y))} \tag{8}$$

where $C(F_X(x), F_Y(y))$ is the bivariate cumulative probability calculated by the copula and $F_X(x)$ and $F_Y(y)$ are the cumulative probabilities calculated by their marginal CDFs.

In this study, three bivariate cases are considered for the frequency analyses. The first case considers peak discharge and flood volume, the second case considers total rainfall and maximum wind speed, and the third case considers wave height and storm surge. Our framework can also accommodate exploration of other bivariate cases such as flood volume with maximum wind speed. However, these bivariate cases can be constructed only if data are available at geographically close weather stations and stream gauges and such close data points are seldom available. Therefore, we focus here on the three abovementioned bivariate cases.

The parameter θ is estimated for the three bivariate cases. Among four copulas, the optimal copula is selected as the one with the lowest AIC and BIC. Additionally, the optimal copula is verified with K-S test as explained in Subsection 3.2.1.

2.4.3. Trivariate Return Period

The trivariate return period is calculated based on vine copula theory (Brechmann & Schepsmeier, 2013; In Joe & Kurowicka, 2011; Kraus & Czado, 2017). In vine copula theory, a joint CDF is decomposed into the combination of bivariate copula functions. In other words, a vine copula combines bivariate copulas to build a high-dimensional multivariate joint CDF. The most commonly used vine copula structures are the canonical or C-vine structure and drawable or D-vine structure (Aghatise et al., 2021; Nguyen et al., 2021; Shafaei et al., 2017). We use the D-vine structure to estimate the trivariate return period of hurricane events because of its broad range of applicability due to its higher flexibility compared to the C-vine structure (Aas et al., 2009; Daneshkhah et al., 2016). In addition, the D-vine structure is more effective when analyzing mutually correlated variables (Latif & Simonovic, 2022; Sun et al., 2020).

Based on Rosenblatt's transform (Rosenblatt, 1952), the trivariate PDF is given as:

$$f_{XYZ}(x, y, z) = f_X(x) \cdot f_{Y|X}(y|x) \cdot f_{Z|XY}(z|x, y) \tag{9}$$

Here, $f_{Y|X}(y|x)$ and $f_{Z|XY}(z|x,y)$ can be substituted by Equation 10 based on the theory of copula.

$$\begin{aligned} f_{Y|X}(y|x) &= c_{XY}((F_X(x), F_Y(y)) \cdot f_Y(y) \\ f_{Z|XY}(z|x, y) &= c_{YZ|X}((F_{Y|X}(y|x), F_{Z|X}(z|x)) \cdot c_{XZ}((F_X(x), F_Z(z)) \cdot f_Z(z) \end{aligned} \tag{10}$$

Combining the above equations, the trivariate PDF can be expressed as:

$$\begin{aligned} f_{XYZ}(x, y, z) =& f_X(x) \cdot f_Y(y) \cdot f_Z(z) \cdot c_{XY}((F_X(x), F_Y(y)) \cdot c_{XZ}((F_X(x), F_Z(z)) \\ & \cdot c_{YZ|X}((F_{Y|X}(y|x), F_{Z|X}(z|x)) \end{aligned} \tag{11}$$

Equation 10 is the trivariate PDF for a structure where X is in center. In the structure where Y and Z are centered, the trivariate PDF is determined via Equation 12.

$$\begin{aligned} f_{Y-\text{center}}(x, y, z) &= f_X(x) \cdot f_Y(y) \cdot f_Z(z) \cdot c_{XY}((F_X(x), F_Y(y)) \cdot c_{YZ}((F_Y(y), F_Z(z)) \\ &\quad \cdot c_{XZ|Y}((F_{X|Y}(x|y), F_{Z|Y}(z|y)) \\ f_{Z-\text{center}}(x, y, z) &= f_X(x) \cdot f_Y(y) \cdot f_Z(z) \cdot c_{XZ}((F_X(x), F_Z(y)) \cdot c_{YZ}((F_Y(y), F_Z(z)) \\ &\quad \cdot c_{XY|Z}((F_{X|Z}(x|z), F_{Y|Z}(y|z)) \end{aligned} \tag{12}$$

The trivariate exceedance probability can be calculated by integrating the derived PDF with target values (x, y, z) as follows.

$$P(X > x, Y > y, Z > z) = \int_x^\infty \int_y^\infty \int_z^\infty f(x, y, z) dx dy dz \tag{13}$$

The trivariate return period is the reciprocal of the exceedance probability calculated in Equation 13.

Trivariate frequency analyses are demonstrated in two cases. In the first case, we analyze the annual maximum series of peak discharge, total rainfall depth and maximum wind speed. In the second case, we examine the annual maximum series of total rainfall depth, maximum wind speed and wave height. As there are four variables to consider, one needs to be excluded for each trivariate analysis. To decide which variable to exclude, we calculate and compare their variance inflation factor (VIF). The variable with highest VIF is excluded to avoid multicollinearity issue (Folli et al., 2020; Lindsey & Sheather, 2010; Tay, 2017). In the first case, the flood volume has a higher VIF than the other three variables; hence it is omitted from the trivariate frequency analysis. In the second case, the storm surge has the highest VIF among the variables, so it is excluded from the trivariate frequency analysis.

The three variables can be composed of three D-vine structures and each structure is classified according to the variable located in the center. For example, structures in which the total rainfall depth, flood volume and maximum wind speed is in the center are denoted as are R-centered, Q-centered and W-centered, respectively. Figure S1 in Supporting Information S1 shows constructions of three D-vine structures with peak discharge, total rainfall depth, and maximum wind speed.

The black rectangle represents a variable and the white circle represents the copula function. That is, the second line, the copula, is constructed using two variables in the first line. The third line shows the conditional non-exceedance probabilities calculated with the copula in the second line. Then, the copula in the fourth line can be constructed by combining the two conditional non-exceedance probabilities; through this, the trivariate exceedance probability can be calculated.

The parameter θ is estimated consistent with our bivariate frequency analyses. The best copula is selected based on AIC and BIC. Also, the K-S test is performed with the selected copula.

3. Study Area

We demonstrate the framework on Hurricane Ian that occurred in October 2022. Hurricane Ian gathered strength over the warmer-than-normal waters of the Caribbean and in an environment of abundant moisture and light winds. Ian tracked northward over Western Cuba as a category 3 hurricane and then continued north, intensified further, before making landfall south of Punta Gorda, Florida. The hurricane brought dangerous storm surge, meters of rain, and category 5 winds to Florida and damaged buildings, trees, and public facilities. Ian had a huge impact on many cities in Florida, including Orlando, Sanford, and Melbourne. In addition, numerous structures, including the Sanibel Causeway and bridge to Pine Island were destroyed by the storm surge (Baker & Osorio, 2022; Treisman, 2022). Despite substantial damages throughout western Cuba and across the southeast United States, more than 95% of the casualties occurred in Florida. Therefore, we selected Florida as a study area for the frequency analyses of this hurricane event.

3.1. Data Preparation

We collected data on four variables: rainfall, flow discharge, wind speed and sea level. Local climatological data provided by NOAA's National Center for Environmental Information (NCEI) are used for hourly rainfall and wind speed (NOAA NCEI, 2017), while data provided by USGS' National Water Information System (NWIS) are used for hourly flow discharge (USGS NWIS, 2016). Data provided by NOAA's National Ocean Service (NOS) are used for hourly sea level (NOAA NOS, 2020).

For the spatial analyses, we collected observed data from weather stations, stream gauges and tidal gauges with more than 30 years of record. Of the 1,411 stream gauges, 93 weather stations and 21 tidal gauges in Florida, only 53 stream gauges, 13 weather stations and 10 tidal gauge have sufficient data; these were chosen for our frequency analyses (Figure 2).

For the point-based analyses, we identified weather stations, stream gauges and tidal gauges that are: (a) located in area affected by Hurricane Ian; and (b) close to each other as defined by the same HUC8 basin. We found only two cases that meet these criteria: (a) Daytona Beach International Airport station from NOAA and Tomoka River near Holly Hill gauge from USGS; and (b) Key West International Airport station from NOAA and Key West tidal gauge form NOAA. From these stations and gauge, total rainfall depth, maximum wind speed, peak discharge, flood volume, wave height and storm surge for Hurricane Ian are extreme and used for the point-based

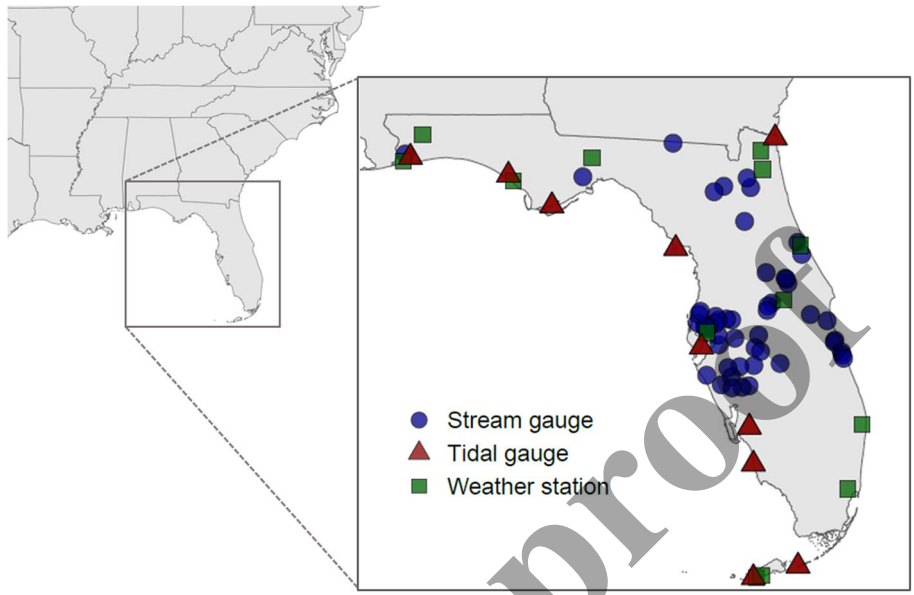

Figure 2. Selected weather stations, stream gauges, and tidal gauges across the study area, Florida.

analyses. The distance between the first trivariate case is approximately 5.8 km, both belonging to the same HUC8 basin, Daytona-St. Augustine Basin (HUC 03080201). The distance between the second trivariate case is approximately 5.3 km, both belonging to the same HUC8 basin, Florida Bay-Florida Keys Basin (HUC 03090203).

Rainfall and wind speed data from the Daytona Beach International Airport and Key West International Airport stations have been observed since 1 January 1948, and flow data at Tomoka River near Holly Hill stream gauge have been measured since 1 October 1986. Sea level data at Key West tidal gauge have been measured since 1 January 1943. Therefore, frequency analyses are performed using 35-year data from 1 January 1987 to 31 December 2021, which is their common observation period. Observed data in 2022 are excluded for frequency analyses and used separately to calculate the return period of Hurricane Ian.

Frequency analyses are performed for events using rainfall, wind speed, flow discharge, and sea level data. We define an event for each variable as follows. For rainfall, an event can be determined by the concept of inter-event time definition (IETD) and threshold (USEPA, 1986). This study applies 10 hr of IETD and 5 mm of threshold to define a rainfall event based on recommendations from previous studies (Guo & Baetz, 2007; Hassini & Guo, 2016). Then, each rainfall event can be characterized with its total depth and duration. The maximum wind speed for each event is calculated by selecting maximum hourly wind speed during the rainfall period. For flow discharge, we separate the baseflow for each event. The direct runoff and baseflow of the streamflow data is separated by applying the recursive digital filter (Eckhardt, 2005). Finally, the flood event can be prepared with direct runoff of the flow discharge data. In the case of a flood event, both peak discharge and flood volume are used for the analyses. For sea level, wave height is generally considered as raw sea level and storm surge is defined with sea level minus astronomical tide (Quinn et al., 2014; Shimura et al., 2022; Vousdoukas et al., 2016). Thus, we calculate astronomical tide using harmonic constituents provided by NOAA gauges. Then, storm surge time series are generated by separating astronomical tide from sea level data.

The block maxima approach is applied to sample annual maximum series from rainfall events, flood events and sea level data. For all cases, we consider two variables for selecting annual maximum series. For the rainfall events, total rainfall and maximum wind speed are considered, while peak discharge and flood volume are used for choosing annual maximum series. Wave height and storm surge are used for choosing annual maximum series of sea level time series. Exceedance probability of each event is calculated using non-parametric empirical copula method. For a given year, the event with the highest exceedance probability is selected as the annual maximum event in our analyses. From 1992 to 2021, a total of 30 annual maximum series from 53 stream gauges (for peak flow and flood volume), 13 weather stations (for total rainfall depth and maximum wind), and 10 tidal gauges (for wave height and storm surge) are determined for the spatial analyses (Figure 3).

Among the 53 stream gauges, the maximum flood volume during Hurricane Ian is 192.0 Mm^3, the largest volume in our period of record. Peak discharge of Hurricane Ian is measured as 390.7 m^3/s, the second highest after that of Hurricane Irma in 2017. However, the total rainfall depth, maximum wind speed, wave height and storm surge associated with Hurricane Ian appear to be less extreme than the flow characteristics.

Figure S2 in Supporting Information S1 illustrates the annual maximum series from 1987 to 2021 and the characteristics of Hurricane Ian in Daytona Beach International airport station and Tomoka River Near Holly Hill stream gauge. Total rainfall depth, maximum wind speed, peak discharge, and flood volume of Hurricane Ian are higher than most of the historical annual maximum series. The total rainfall and maximum wind speed of Hurricane Ian are the second highest at Daytona Beach International airport station with 333.5 mm and 23.7 m/s, respectively. For peak flow and flood volume, Hurricane Ian recorded 61.9 m^3/s and 7.2 Mm^3 in Tomoka River Near Holly Hill stream gauge as the greatest values. Consequently, these data indicate that Hurricane Ian caused rare extreme wind, rain and flood conditions in this area.

Figure S3 in Supporting Information S1 displays the annual maximum series from 1987 to 2021 along with the features of Hurricane Ian at Key West International Airport station and Key West tidal gauge. Hurricane Ian's total rainfall and maximum wind speed are 167.4 mm and 21.6 m/s, respectively. For wave height and storm surge, Hurricane Ian recorded as 2.9 and 1.9 m at Key West tidal gauge. The maximum wind speed in Key West is the second highest, and both wave height and storm surge are also the second highest on record. As a result, this information shows that Hurricane Ian also generated extreme wind, rainfall, and sea level conditions in near Key West.

4. Results

4.1. Univariate Frequency Analyses

The procedure of applying univariate frequency analysis is demonstrated using data from Daytona Beach International Airport weather station and Tomoka River Near Holly Hill stream gauge. Annual maximum series of four independent variables—total rainfall, maximum wind speed, flood volume and peak discharge—are constructed and fit with the GEV distribution.

Table S1 in Supporting Information S2 shows the parameters of GEV distribution estimated for each variable and p-value of the K-S test. In Table S1 in Supporting Information S2, p-values of all variables are >0.05, suggesting that GEV distribution is statistically significant (5% significance level). Figure 4 shows the histogram and the fitted GEV of the four variables. In Figure 4, the overall shape of the GEV for each variable is visually well aligned with the histogram and the difference of their peak relative frequency is less than 10% of the peak value of the fitted GEV distribution.

Since the return period in the univariate frequency analysis method is the reciprocal of exceedance probability, the return period is calculated with the GEV distribution in Figure 4. First, the total rainfall during Hurricane Ian is 333.5 mm and the exceedance probability is calculated as 0.0255, suggesting a return period of 39.2 years, with a 95% confidence interval ranging from 34.1 to 45.0 years. Following the similar procedure for maximum wind speed, peak discharge, and flood volume, the return periods are calculated as 77.3 years, 60.2 and 85.2 years, respectively. The 95% confidence interval ranges are 54.2–110.1 years, 55.6–65.0 years and 82.1–88.3 years, respectively.

This procedure is repeated for the 53 stream gauges, 13 weather stations, and 10 tidal gauges for the spatial analyses. For all these stations, GEV distribution is confirmed to be a valid choice based on K-S test (0.05 significance level). Figure 5 shows the results of univariate frequency analyses from all weather stations, stream gauges and tidal gauges.

In Figures 5a and 5b, the spatial distribution of return period is different for peak discharge and flood volume. The derived return periods for flood volume are much shorter than those from peak discharge. The spatial average of the return period for peak discharge is 24.2 years, while it is 10.4 years for flood volume. In the case of peak discharge, stream gauges with a high return period (>30-year) show spatial patterns similar to the reported path of Hurricane Ian. However, the spatial pattern from the results of flood volume is unclear and inconsistent with the reported path of Hurricane Ian.

The spatial patterns of return periods from the total rainfall and maximum wind speed are also not consistent with each other. For total rainfall depth, the spatial average of return period is 7.1 years, whereas it is 11.0 years for maximum wind speed. In addition, it is common for weather stations to have large differences between the two return periods. For example, in Key West Naval Air weather station, the return period calculated by total rainfall depth is 8.5 years, whereas that calculated by the maximum wind speed is 43.4 years. Similarly, the return period

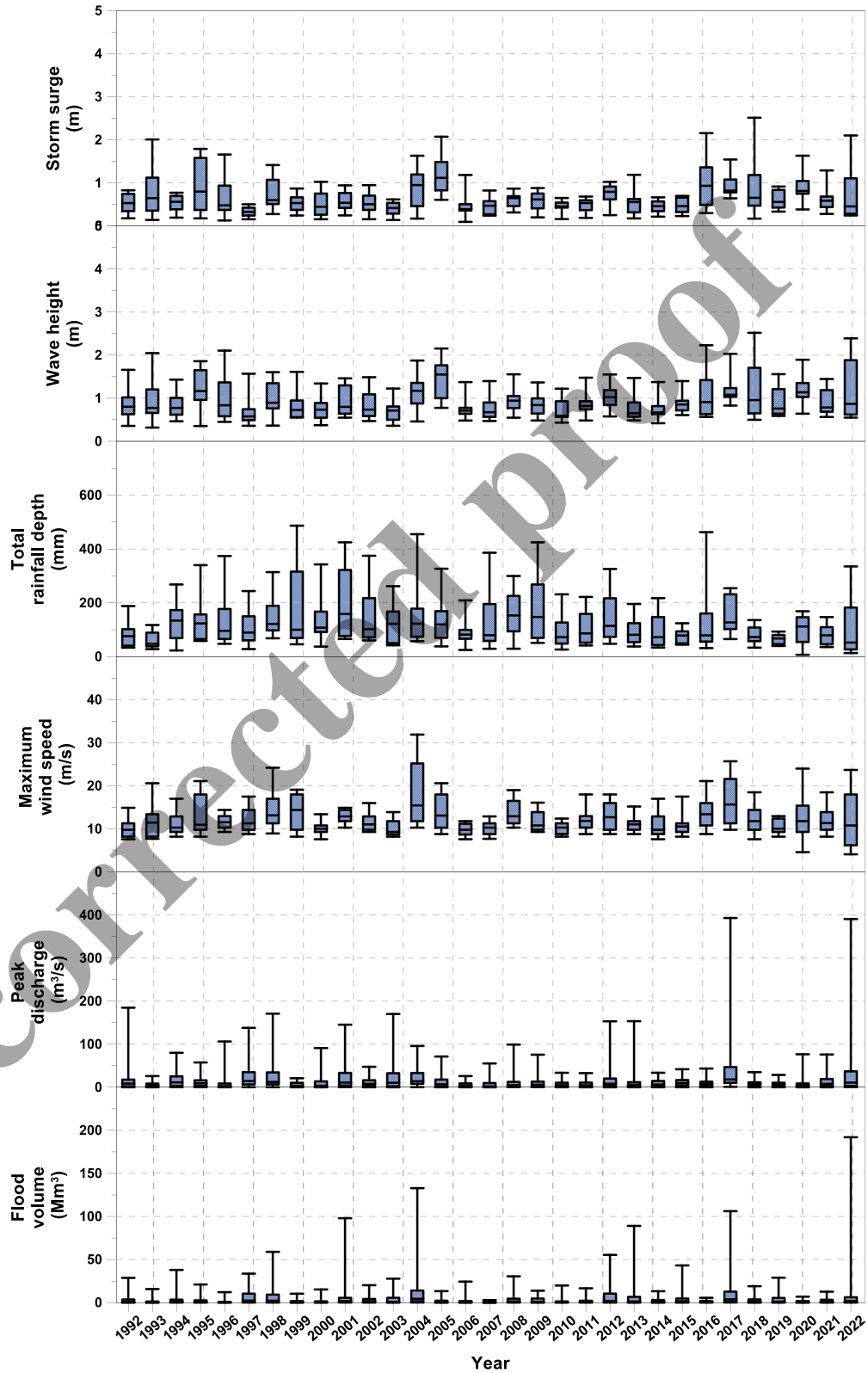

Figure 3. Boxplots derived by annual maximum series from 53 stream gauges, 13 weather stations, and 10 tidal gauges.

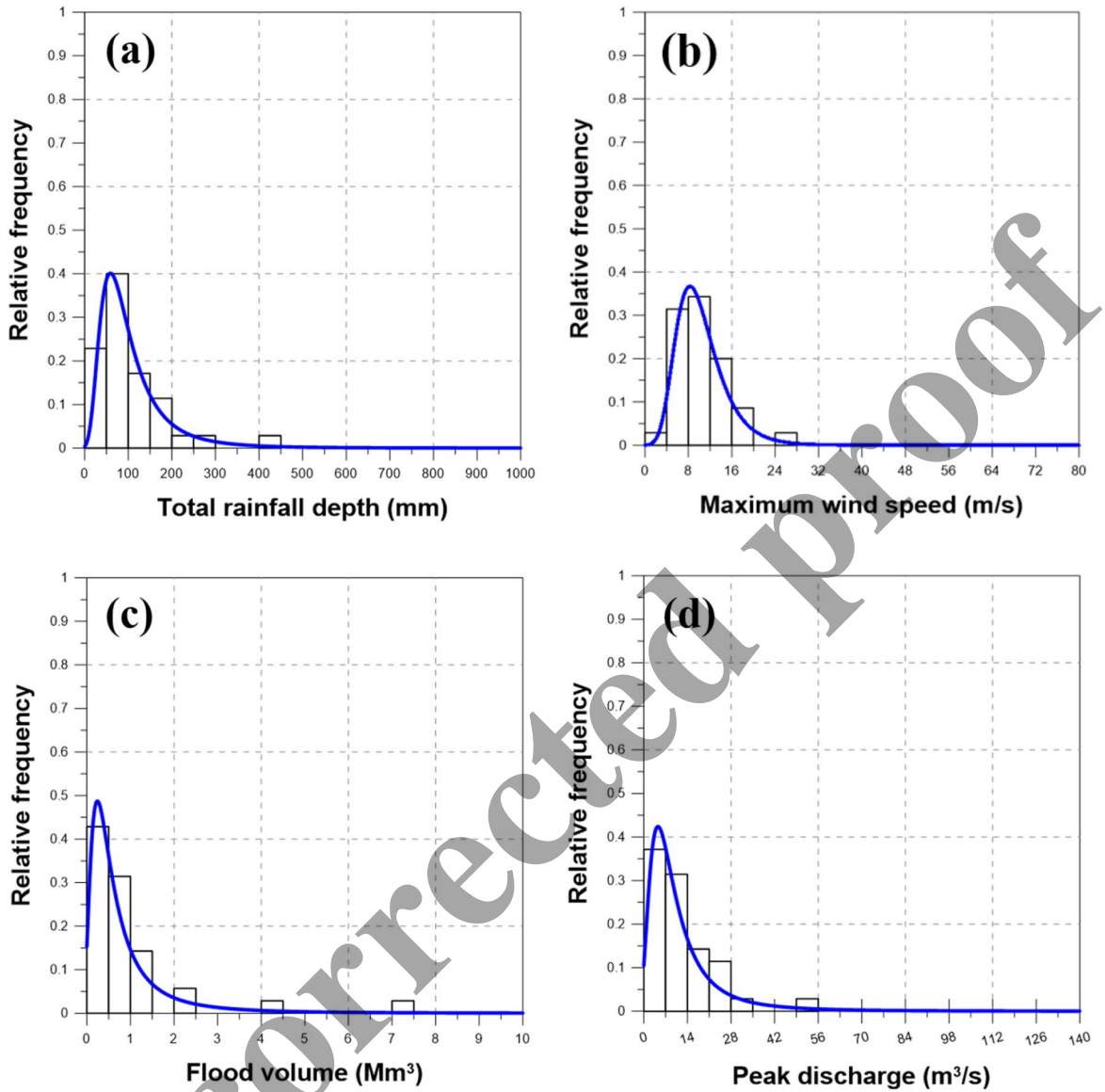

Figure 4. Histogram and probability distribution of (a) total rainfall depth, (b) maximum wind speed, (c) flood volume, and (d) peak discharge.

calculated by total rainfall depth at Orlando International Airport station is only 10.7 years, while the return period calculated by maximum wind speed is 33.8 years.

In contrast to other cases, the return periods for wave height and storm surge show similar spatial patterns as each other. In the case of wave height, the spatial average of return period is 25.2 years, while it is 18.6 years for storm surge. Hurricane Ian predominantly affected the area around Fort Myers. Additionally, the return period of both wave height and storm surge near Key West and Jacksonville are calculated to be >10 years.

Even though the analyses are for the same hurricane, return periods are very different depending on the selected variable. This is the major limitation of univariate frequency analyses that has been identified in previous studies too (Balistrocchi et al., 2017; Muthuvel & Mahesha, 2021; Xiao et al., 2009; Yin et al., 2018).

4.2. Bivariate Frequency Analyses

The bivariate frequency analyses are demonstrated using the same data from Daytona Beach International Airport weather station and Tomoka River Near Holly Hill stream gauge. Figure 6 shows scatter plots of two bivariate cases from the selected weather station and stream gauge. In this figure, the peak discharge and flood volume

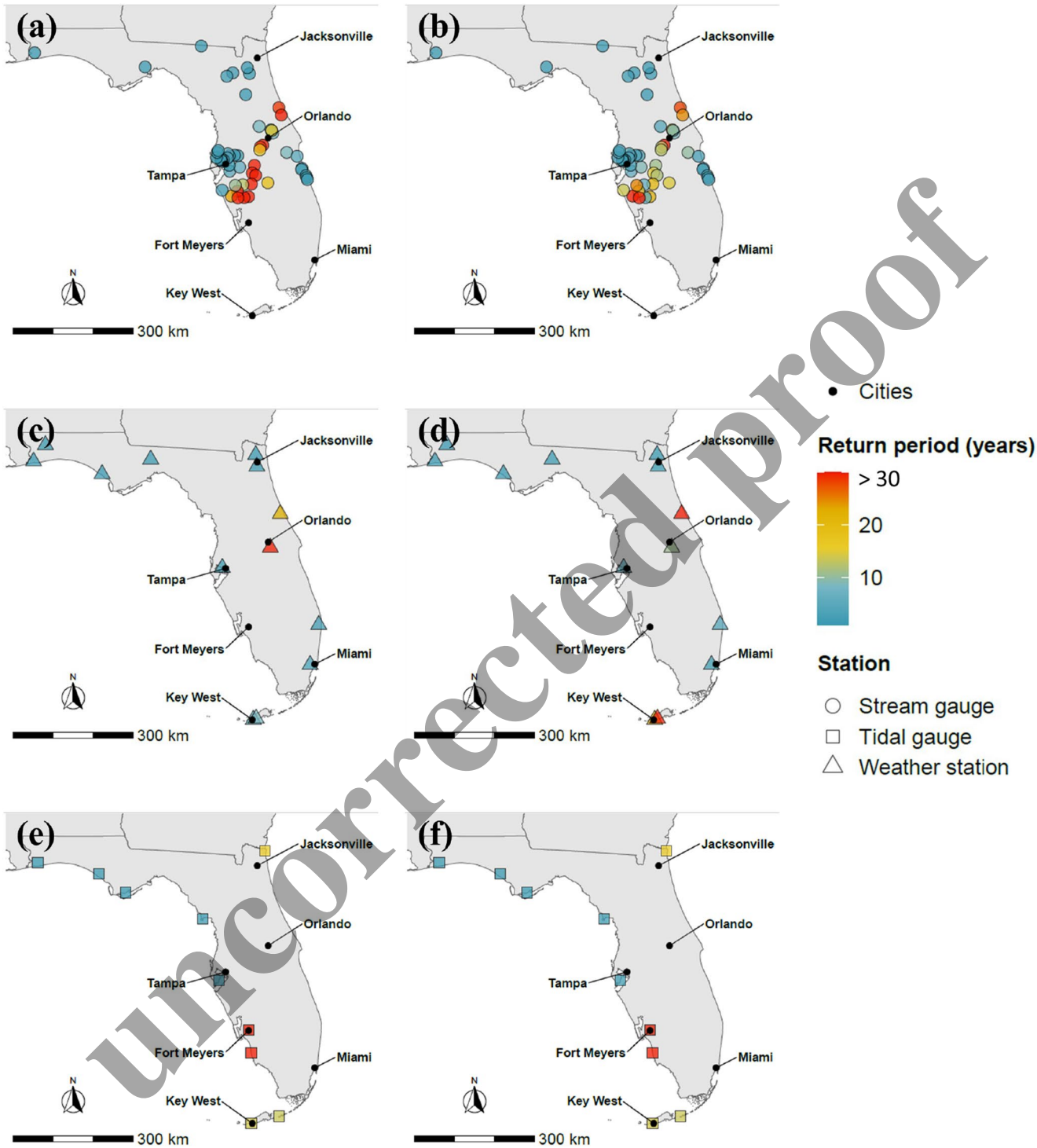

Figure 5. Univariate return period calculated across the study area based on: (a) peak discharge, (b) flood volume, (c) total rainfall depth, (d) maximum wind speed, (e) wave height, and (f) storm surge.

show a strong positive correlation, while maximum wind speed and total rainfall depth have rather a weak positive correlation. For those bivariate cases, parameter estimation is performed for copula candidates by applying MLE. Table 2 summarizes the results of parameter estimation with AIC and BIC.

Among the four copulas, we select the best copula based on AIC and BIC (Table 2). It is found that Clayton copula has the lowest AIC and BIC for peak discharge and flood volume case (AIC < -120 and BIC < -116). In

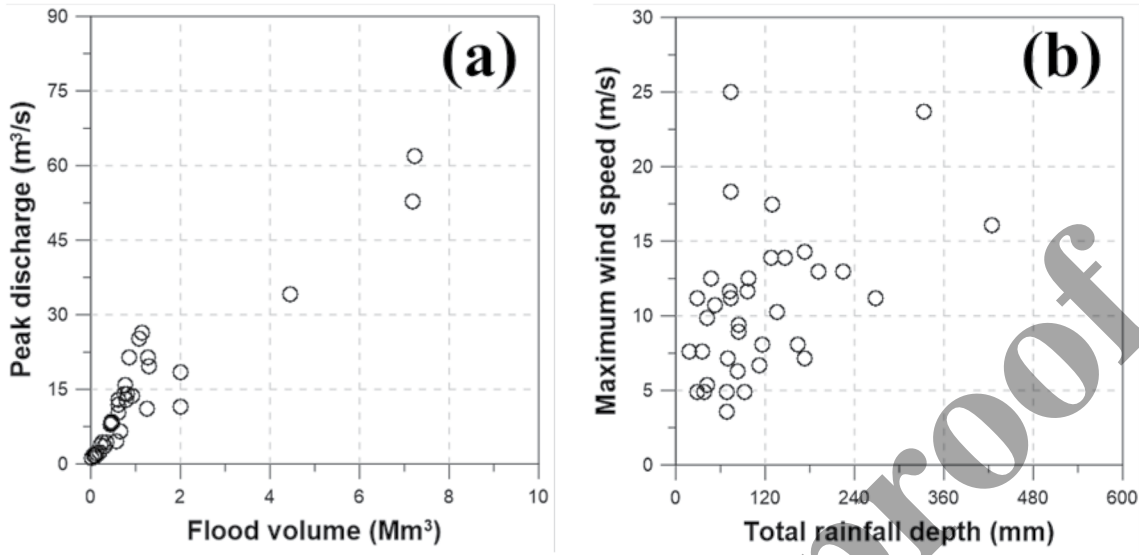

Figure 6. Scatter plots of two cases for bivariate frequency analyses: (a) peak discharge–flood volume, and (b) maximum wind speed–total rainfall depth. Open circles show the annual maximum series from 1987 to 2021. These are based on data from Daytona Beach International Airport weather station and Tomoka River Near Holly Hill stream gauge.

the case of maximum wind speed and total rainfall, the Clayton copula is the one with the lowest AIC and BIC (AIC < −46 and BIC < −42).

The selected copula is further tested with the K-S statistic to evaluate the goodness-of-fit. Figure S4 in Supporting Information S1 is the scatter plot indicating the cumulative probability calculated by the empirical copula and the optimal copula. In Figure S4 in Supporting Information S1, dotted lines represent the critical value to examine the goodness-of-fit of copula. The critical value is calculated as 0.2242 for 35 years of records. All the points from the two bivariate cases are found to be within the upper and lower limits of the K-S test, suggesting that all selected copulas are statistically significant.

Table 2
Parameter Estimations, AIC, and BIC for Bivariate Frequency Analysis Cases, Based on Data From Daytona Beach International Airport Weather Station and Tomoka River Near Holly Hill Stream Gauge

Bivariate case			Peak discharge & flood volume	Maximum wind speed & total rainfall depth
Parameter estimation	Parameter θ	Gumbel	3.887	1.412
		Clayton	5.723	0.937
		Frank	15.672	2.982
		Joe	4.345	1.550
		Gaussian	0.933	0.501
Comparison of fitness	AIC	Gumbel	−114.0	−44.1
		Clayton	**−120.8**	**−46.9**
		Frank	−111.2	−44.2
		Joe	−106.6	−44.6
		Gaussian	−116.7	−44.4
	BIC	Gumbel	−109.3	−39.4
		Clayton	**−116.1**	**−42.2**
		Frank	−106.5	−39.5
		Joe	−101.9	−40.0
		Gaussian	−112.0	−39.7

Finally, the bivariate return periods of Hurricane Ian are calculated with the verified copula. Figure 7 shows the scatter plot and results of bivariate frequency analyses across the study area. This figure provides us with a better understanding of how extreme Hurricane Ian was. Our analyses show that Hurricane Ian has a return period of >500 years in both cases, which are calculated as 824.1 and 1,592.6 years, respectively. Their 95% confidence intervals are computed as 737.4–918.6 years and 974.5–2,593.3 years, respectively. In addition, Figure 7b demonstrates the advantage of bivariate frequency analyses over univariate analyses. In Figure 7b, there are cases where the total rainfall or maximum wind speed is greater than that of Hurricane Ian. However, when both variables are considered, the return period of Hurricane Ian is calculated to be the longest by far. Uncovering these latent characteristics of hurricanes cannot be achieved through univariate analyses alone.

Figure 8 shows the spatial distribution of the estimated bivariate return periods across the study area using annual maximum series from the 53 stream gauges, 13 weather stations and 10 tidal gauges. The path of Hurricane Ian is more apparent in Figure 8 compared to the map based on the univariate results (Figure 5). The bivariate return period map enables us to identify areas that are affected by hurricanes at various return periods. As an example, the return periods at Tampa are relatively low compared to the area south of Tampa to Orlando and Daytona Beach where many weather stations and

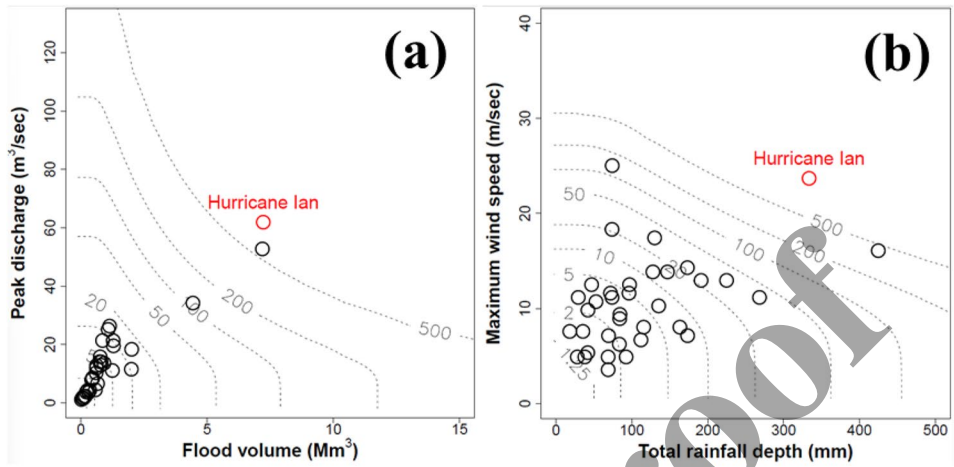

Figure 7. Scatter plots and contours of bivariate return period based on two pair cases: (a) peak discharge–flood volume and (b) maximum wind speed–total rainfall. These are based on data from Daytona Beach International Airport weather station and Tomoka River Near Holly Hill stream gauge.

stream gauges reported high return periods (>30 years). In addition, bivariate return period of tidal gauges near Fort Meyers are much higher than 30 years. Interestingly, bivariate return period >30 years is also found in weather stations near Key West, because of their high maximum wind speed. The number of weather stations, stream gauges and tidal gauges with return periods longer than 30 years is 27 and the spatial average return period of these is 206.9 years.

4.3. Trivariate Frequency Analyses

Peak discharge, total rainfall depth, and maximum wind speed from Daytona Beach International Airport station and Tomoka River Near Holly Hill gauge are used here to demonstrate the trivariate frequency analysis. The analyses are conducted with R-centered, Q-centered, and W-centered D-vine structures. Table S2 in Supporting Information S2 shows the estimated parameters, selected copula and K-S test results used for copula construction for each of the three D-vine structures.

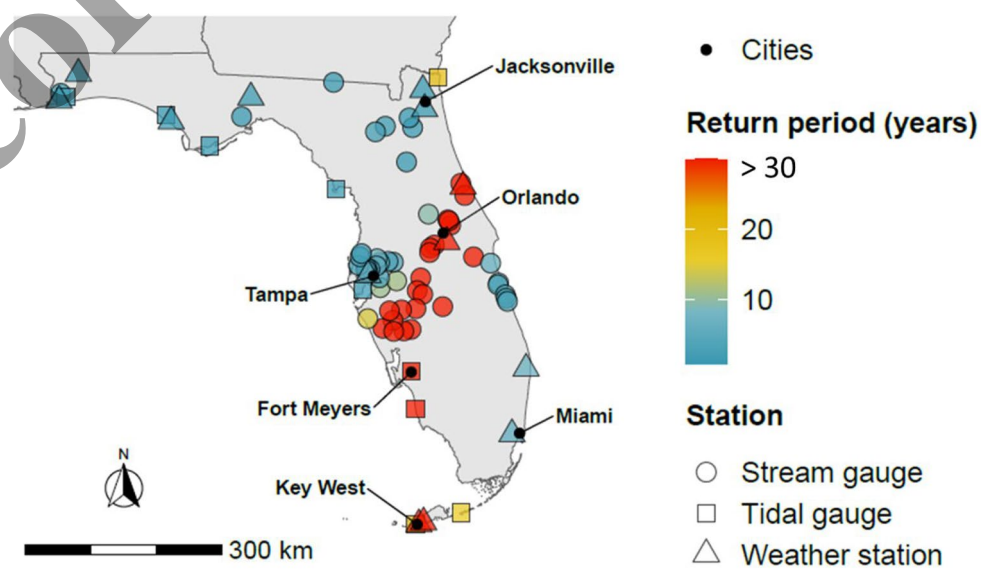

Figure 8. Return period map with bivariate return period from the peak discharge and flood volume of stream gauges (indicated by circles), total rainfall depth and maximum wind speed of weather stations (indicated by triangles) and wave height and storm surge of tidal gauges (indicated by squares).

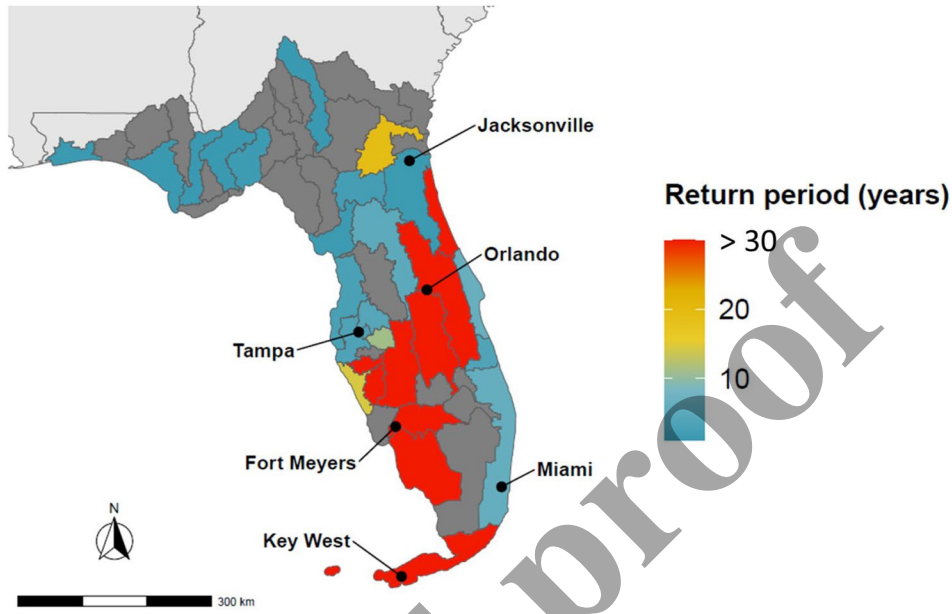

Figure 9. Hurricane Ian's return period map based on the average of three bivariate frequency analysis cases.

The return periods via the trivariate frequency analyses are derived using the constructed copulas and D-vine structure. The return period varies strongly by structure of D-vine tree. When R is centered, the trivariate return period is 332.1 years. The Q-centered return period was 896.48 years, while W-centered return period was 1722.9 years. The 95% confidence intervals for them are calculated to be 216.8–576.0 years, 537.4–1232.8 years, and 866.0–3602.2 years, respectively.

It is found that all trivariate return periods of Hurricane Ian are greater than 300 years. In addition, trivariate return periods follow the same rank order as the univariate return period for the variable located in the center. For example, the variable with the greatest univariate return period is the maximum wind speed, and the W-centered trivariate return period is also the greatest. The lowest return period is also found from the total rainfall case of the univariate analyses and R-centered structure of the trivariate analyses.

4.4. Spatial Pattern of Hurricane Ian's Return Period

The spatial pattern of the return period of Hurricane Ian is generated by averaging the results of our bivariate frequency analyses. We use HUC8 boundaries as the base map for hurricane return period map. For each HUC8 basin, the average of bivariate return period is calculated using stream gauges or weather stations or tidal gauges located in that area. Figure 9 shows the hurricane return period map based on the results of bivariate frequency analyses.

Among the 50 HUC8 basins in Florida, nine basins have an average return period >30 years, while 19 basins have an average return period of <20 years. Orlando is the only large population center with a high average return period (>30 years). Other large population centers—Jacksonville, Tampa, and Miami—are located in counties with lower average return periods (<20 years).

The Sarasota Bay Basin has a bivariate return period of 14.4 years, even though it is in the path of Hurricane Ian. This is due to the low univariate return period of peak discharge variable, which is only 2.1 years and is likely not representative of the multivariate return period. If we were able to analyze rainfall and wind characteristics for this basin, we would likely determine a longer return period. Unfortunately, there are no weather stations in this basin with at least 30 years of observations. This indicates the importance of multivariate frequency analyses considering rain, wind speed, and flood variables together.

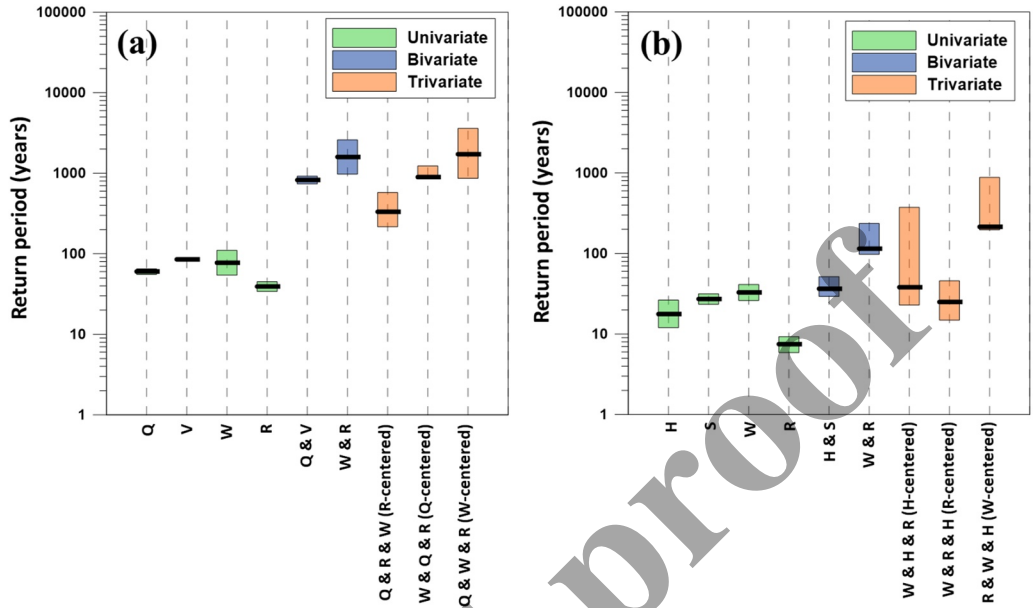

Figure 10. Comparison of univariate, bivariate, and trivariate return periods of Hurricane Ian in (a) Daytona-St. Augustine Basin and (b) Florida Bay-Florida Keys Basin. *Q*, *V*, *W*, *R*, *H* and *S* represent peak discharge, flood volume, maximum wind speed, total rainfall depth, wave height and storm surge.

5. Discussion

5.1. Comparisons of the Estimated Return Periods and Interpretations

This study conducts a comparative analysis of point-based return periods within two specified basins—the Daytona-St. Augustine basin and the Florida Bay-Florida Keys Basin. The results of the three frequency analysis methods—univariate, bivariate and trivariate—are compared and their implications are discussed. Figure 10 summarizes all return periods and their 95% confidence intervals of Hurricane Ian calculated by applying the three frequency analysis methods. In Figure 10, the terms R-centered, Q-centered, W-centered, and H-centered refer to the configuration of trivariate analysis structures where *R*, *Q*, *W*, and *H* is positioned at the center.

Figure 10 shows a large variability in the return period estimates depending on the frequency analysis method and the selected variable(s). It should be noted that the results from different frequency analysis methods—univariate, bivariate, or trivariate—are not directly comparable (Serinaldi, 2015; Volpi et al., 2015) because the values of return period are significantly dependent on the applied methodology. However, by comparing their magnitudes depending on the selected variable(s) in the same frequency analysis method, we can gain a fuller picture of the characteristics and implications of the estimated return periods.

First, the results of Daytona-St. Augustine Basin show that selection of flood volume led to the greatest return period (85.2 years) in the univariate frequency analysis method. However, pairing this variable with peak discharge does not lead to the greatest return period estimated through bivariate frequency analyses. In the case of bivariate frequency analysis method, the combination of total rainfall depth and wind speed yields the greatest return period (1,592.6 years). In other words, the estimated return period of Hurricane Ian via the combination of total rainfall depth and maximum wind speed leads to more conservative return period than using the two flood variables. Further, the trivariate frequency analyses indicate that Hurricane Ian had an extremely high wind speed, with the greatest return period in the case of a W-centered structure (using maximum wind speed as the central variable).

The results of Florida Bay-Florida Keys Basin show that the return period of total rainfall depth is the lowest (7.5 years) in the univariate frequency analysis method. However, its combination with maximum wind speed yields to the greatest bivariate return period as 114.9 years, because of the greatest univariate return period of maximum wind speed (32.9 years). Additionally, the trivariate frequency analyses reveal that Hurricane Ian had an exceptionally high wind speeds, with the greatest return period in the case of a W-centered structure (using maximum wind speed as the central variable).

According to the comparison of confidence intervals, the intervals become wider as more variables are considered for the frequency analyses. For univariate, bivariate, and trivariate analyses, the average length of the confidence intervals is 20.6 years, 900.0 years, and 1263.6 years from the results of Daytona-St. Augustine Basin. The results of Florida Bay-Florida Keys Basin also have 10.3 years, 80.2 and 355.9 years of average length of the confidence intervals for univariate, bivariate, and trivariate analyses. It is important to note that bivariate and trivariate analyses yield great return periods, but their uncertainty is also high. It may also be referred to as the uncertainty caused by the limited years (35 years) of historical data, which is much shorter than the calculated return periods from the bivariate and trivariate analyses.

Furthermore, it is found that the confidence intervals including maximum wind speed are wider than other intervals in both the Daytona-St. Augustine Basin and Florida Bay-Florida Keys Basin. For example, among the results of the univariate frequency analyses, the length of the confidence interval for wind speed is the widest (55.9 and 15.1 years). The confidence interval for the bivariate case with maximum wind speed (1,618.8 and 138.2 years) is much wider than the other case (181.2 and 22.2 years). In our trivariate frequency analyses, W-centered results have the widest confidence interval (2736.2 years and 684.3 years). Although the maximum wind speed clearly shows the extremes of Hurricane Ian, the results with that data are subject to the highest level of uncertainty.

This study has demonstrated the high sensitivity of return period to the type of analysis and the combination of hurricane hazard variables included. This raises the broader question of which method is more suitable or reliable for risk management. Answering this question would necessarily involve study of the specific information needs and decision-making contexts of risk managers. For example, insurance companies that only insure wind losses may focus on univariate wind risk, whereas emergency managers may desire inclusion of flood measures, both surge and inland flooding. The important interdisciplinary work required to understand the societal integration of the multiple analysis methods presented here is recommended for future research.

Our method is complementary to existing approaches to risk quantification. FEMA, for example, uses a variety of risk assessment tools to quantify hurricane risk with emphasis on wind and flood. FEMA's Hazus Hurricane Model, for example, represents a class of risk assessment models that quantifies primarily hurricane wind risk based on large samples of synthetic hurricane events (FEMA, 2022). These synthetic events are based on large Monte Carlo sampling of historical data to generate robust return periods. While our approach is based on a small observational data size and may suffer from larger uncertainty bounds, our method includes additional hurricane risk variables in a manner that retains physical consistency between all considered hurricane variables.

To demonstrate how our results compare with an existing risk assessment, we provide here a comparison of rainfall with the NOAA Atlas 14 point precipitation frequency estimates (Perica et al., 2013). First, at Daytona Beach International Airport weather station, total rainfall depth and duration are 333.5 mm and 43 hr, respectively, during Hurricane Ian period. According to by Perica et al. (2013), the return period for this event, was estimated to be from 50 to 100 years when considering a fixed duration of 48 hr. In contrast, our univariate return period is calculated to be 39.2 years. Second, the rainfall event is characterized by a 52-hr duration and a 167.4 mm total rainfall depth at the Key West International Airport weather station. Perica et al. (2013) provided its return period from 2 to 5 years when using a fixed duration of 48 hr, while our univariate return period is calculated as 7.5 years. It should be noted that the rainfall duration at the Daytona Beach International Airport weather station (43 hr) is shorter than the fixed duration provided by NOAA (48 hr), while the duration in Key West International Airport weather station (52 hr) is longer than NOAA's fixed duration (48 hr). Consequently, a direct and accurate comparison between our results and estimates by Perica et al. (2013) is not possible due to these differences in rainfall duration. This highlights the primary limitation of the existing method, which does not offer continuous rainfall durations for estimating return periods.

In addition, we are not aware of any prior studies that estimate Hurricane Ian's return period. Thus, we compare our results with those by previous studies estimating the return period of major hurricanes, which have the same wind speed-based category as Hurricane Ian (category 5). Hurricane Katrina's return period was estimated <100 years (Elsner et al., 2006; Grinsted et al., 2012; Parisi & Lund, 2008) based on univariate frequency analyses on wind speed, central pressure and storm surge. Its return period was also calculated to exceed 100 years, 112.4 years by Needham et al. (2012) and 111.0 years Resio et al. (2009) based on univariate frequency analyses on storm surge. Another category 5 hurricane, Hurricane Maria's return period was also estimated as 115 years by Keellings and Hernández Ayala (2019) based on univariate frequency analyses on precipitation. The return period of Hurricane Irma ranged from 110 to 283 years (Bacopoulos, 2019) based on univariate frequency analyses on

sea levels. Although most return period estimates were <1,000 years, there were cases where even a Category four hurricane, like Hurricane Harvey, had an estimated return period >1,000 years (Nyaupane et al., 2018; Sebastian et al., 2017) based on univariate frequency analyses on peak discharge and precipitation, and >9,000 years (van Oldenborgh et al., 2017) based on univariate frequency analyses on precipitation. These discrepancies are caused by unique physical mechanisms of each hurricane and the frequency analysis method. Given the wide range of return period estimated for hurricane event, our results for Hurricane Ian can be considered valid within this context.

5.2. Limitations and Future Research

The granularity of the spatial analyses is limited by the scarcity of weather stations, stream gauges and tidal gauges for the multivariate frequency analyses. Among the 53 stream gauges, 13 weather stations and 10 tidal gauges considered here, there are only two cases that can be coupled for the multivariate analyses. Other gauges and stations are not affected by Hurricane Ian or are not located in the same HUC8 basin. This hinder us from performing comprehensive spatial trivariate frequency analyses. Further applications of the framework can extend to other datasets beyond our study area to conduct additional trivariate frequency analyses. However, the presented trivariate analyses for the case of Daytona Beach and Key West can serve as an example for hurricanes in other locations where such data are available. Our goal here was to demonstrate the approach with the expectation of further verification and development as the number of additional analyses increases.

Another limitation of this study is that it does not consider other environmental compounding factors of hurricane risk beyond rainfall, wind speed, flow discharge and sea level. These factors, such as groundwater (which is very shallow in most of South Florida that was impacted by Hurricane Ian) should be analyzed alongside rainfall, wind speed, flow discharge and sea level. We were not able to incorporate these variables because of a lack of readily available data.

As a future study, various combinations of bivariate analyses can be calculated and compared. In fact, there are three combinations of bivariate cases with the six independent variables considered here. In addition, there are other concepts of bivariate return period other than AND concept, such as OR concept, conditional concept, and survival Kendall's return period (Salvadori et al., 2013). Since the authors are not aware of prior work estimating return period of hurricanes with these various concepts, it would be novel to conduct research to compare them with our framework.

The presented approach to estimate the return period of a hurricane event is based on the assumption of a stationary climate. As discussed earlier, climate change and subsequent changes in weather patterns and sea levels are driving nonstationary behavior. Addressing this issue, Bracken et al. (2018) conducted nonstationary multivariate hydrologic frequency analyses, which focused on temporal changes and complex interdependencies among hydrologic variables. Other researchers also applied nonstationary frequency analysis methods (e.g., Kwon & Lall, 2016; Obeysekera & Salas, 2016; Villarini et al., 2009). To improve our framework, this nonstationary frequency analysis method can be incorporated in future study.

Another future study will be to develop hurricane hazard indices based on the results of our frequency analyses. For example, Rezapour and Baldock (2014) developed a hurricane hazard index that estimated hurricane severity by considering factors such as wind, rainfall, and storm surge characteristics. Additionally, Song, Alipour, et al. (2020) and Song, Duan, and Klotzbach (2020) introduced a multi-hazard hurricane index based on the joint probability of rainfall and wind speed associated with Atlantic tropical cyclones in the US. Using our univariate, bivariate, and trivariate frequency analysis methods, an advanced hurricane hazard index may be developed, which would provide a comprehensive, relevant, and accurate assessment of hurricane-related risks.

Finally, our frequency analyses on historical data are not constrained to only include hurricane conditions. Particularly, in years without a hurricane event at a given location, the annual maximum values may be contributed by other weather systems such as strong frontal passages. Since the return period of Hurricane Ian is estimated using these annual maximum series, there may be uncertainties associated with these factors. The data distribution shapes may be dependent on the contributing weather systems. This presents an opportunity to combine our statistical framework with an understanding of the driving physical processes to build new frequency analysis methods to better quantify and understand the return periods. New methods may also consider incorporating physical constraints to the fitted distributions to better inform tail behavior in

the absence of long data records. The data scarcity problem may also be approached through the inclusion of large synthetic hurricane datasets such as provided for wind by the Synthetic Tropical cyclOne geneRation Model (STORM; Bloemendaal et al., 2020) and for rainfall by the TC rainfall model (Lu et al., 2018). Harr et al. (2022) demonstrated the value of using such large synthetic datasets for bivariate hurricane risk analyses.

6. Summary and Conclusions

This study developed and proposed a new framework for calculating multivariate return periods of hurricanes using event-based approach. The point-based and spatial analysis of Hurricane Ian was conducted to verify the applicability of the proposed framework. Using GEV and copula, we performed univariate, bivariate, and trivariate frequency analyses on annual maximum series of flood volume, peak discharge, total rainfall depth, maximum wind speed, wave height and storm surge. For point-based analyses, this study selected representative two cases and annual maximum series from 1987 to 2021 were analyzed. In the case of spatial analyses, annual maximum series from 1992 to 2021 were secured from 53 stream gauges, 13 weather stations and 10 tidal gauges, which are all located in Florida.

The novelty of this study can be summarized as follows. First, our research presents event-based frequency analyses for assessing hurricane risks, providing a more realistic perspective compared to conventional methods which rely on the point times of observation. Second, by encompassing a broader range of variables, such as precipitation, wind speed, flow discharge and sea level, our approach offers a comprehensive assessment of hurricane risks. Third, our framework expands upon existing methods by incorporating various frequency analysis method (i.e., univariate, bivariate and trivariate analyses method) and consistently applying these approaches at an hourly time scale. This innovation allows for a deeper understanding of hurricane risks and more detailed insights into its effects. The notable conclusions of this study can be summarized as follows.

1. This study demonstrated that the framework of event-based frequency analyses can be employed to calculate the multivariate return periods of hurricane events. As part of this framework, block maxima methods were applied to sample annual maximum series. After that, GEV distribution, general copula and D-vine copula were used for return period calculation. Using this framework, multivariate return periods and their maps for Hurricane Ian can be derived.
2. Through point-based analyses, our framework was shown to be applicable for the calculation of multivariate return periods. In the Daytona-St. Augustine Basin, univariate return periods were calculated from 39.2 to 60.2 years. Bivariate return periods for this basin were estimated from 824.1 to 1592.6 years, while trivariate return periods ranged from 332.1 to 1722.9 years. In the Florida Bay-Florida Keys Basin, univariate return periods were estimated from 7.5 to 32.9 years. Bivariate return periods for this basin ranged from 36.5 to 114.9 years, and trivariate return periods were calculated from 25.0 to 214.8 years.
3. Through the framework of spatial analyses, we were able to generate a new return period map for Hurricane Ian. In these analyses, the return period map of Hurricane Ian was created based on the results of bivariate frequency analyses. Among the 50 HUC8 basins in Florida, nine had an average return period of >30 years, while 19 basins had an average return period of <20 years. Orlando was the only large city with the average return period of >30 years.

Based on our results, it can be shown that multivariate return periods and return period maps can be generated using the proposed framework. However, we also identified several sources of uncertainty. First, the length of the data for point-based analyses was 35 years, which is much lower than the calculated return periods from bivariate and trivariate analyses. Additionally, the framework for estimating the return period of a hurricane event is based on the assumption of stationarity, which is another source of uncertainty. Furthermore, there is a possibility that other weather systems may affect the annual maximum series used to estimate Hurricane Ian's return period.

Nevertheless, we believe that the results of this study provide disaster responders and managers with valuable insights and useful information. The new hurricane return period map can be useful for disaster response and recovery efforts. Emergency response personnel and managers, such as FEMA and state emergency management departments in the United States, will be able to use the map to prioritize response efforts. Our results may also help climate resilient finance by providing return period maps to help financial risk managers understand their losses and exposures to future events.

Data Availability Statement

Hourly rainfall and wind speed data provided by NOAA's NCEI is available at: https://www.ncdc.noaa.gov/cdo-web/datasets/LCD/locations/FIPS:12/detail.

Hourly flow discharge data (streamflow) provided by USGS' NWIS is available at https://waterdata.usgs.gov/nwis/uv?referred_module=sw&state_cd=fl&format=station_list&group_key=NONE.

Hourly sea level data (mean sea level) provided by NOAA's NOS is available at https://tidesandcurrents.noaa.gov/map/index.html?region=Florida.

Acknowledgments
Ebrahim Ahmadisharaf was partially supported through award No. 2203180 by the United States National Science Foundation (NSF). James Done was supported by the WTW Research Network. The National Center for Atmospheric Research is sponsored by NSF.

References

Aas, K., Czado, C., Frigessi, A., & Bakken, H. (2009). Pair-copula constructions of multiple dependence. *Insurance: Mathematics and Economics*, *44*(2), 182–198. https://doi.org/10.1016/j.insmatheco.2007.02.001

Adams, B. J., & Papa, F. (2001). Urban stormwater management planning with analytical probabilistic models. *Canadian Journal of Civil Engineering*, *28*(3), 545. https://doi.org/10.1139/l01-008

Aghatise, O., Khan, F., & Ahmed, S. (2021). Reliability assessment of marine structures considering multidimensional dependency of the variables. *Ocean Engineering*, *230*, 109021. https://doi.org/10.1016/j.oceaneng.2021.109021

Akaike, H. (1974). A new look at the statistical model identification. *IEEE Transactions on Automatic Control*, *19*(6), 716–723. https://doi.org/10.1109/tac.1974.1100705

Alaya, M. B., Zwiers, F., & Zhang, X. (2020). An evaluation of block-maximum-based estimation of very long return period precipitation extremes with a large ensemble climate simulation. *Journal of Climate*, *33*(16), 6957–6970. https://doi.org/10.1175/jcli-d-19-0011.1

Alipour, A., Yarveysi, F., Moftakhari, H., Song, J. Y., & Moradkhani, H. (2022). A multivariate scaling system is essential to characterize the Tropical Cyclones' risk. *Earth's Future*, *10*(5), e2021EF002635. https://doi.org/10.1029/2021ef002635

Bacopoulos, P. (2019). Extreme low and high waters due to a large and powerful tropical cyclone: Hurricane Irma (2017). *Natural Hazards*, *98*(3), 939–968. https://doi.org/10.1007/s11069-018-3327-7

Baker, L., & Osorio, C. (2022). *Ian cut off residents of Florida's Pine Island. They are just now taking stock*. NPR. Retrieved from https://www.npr.org/2022/10/04/1126806790/pine-island-matlacha-residents-return-hurricane-ian-florida

Balaguru, K., Foltz, G. R., & Leung, L. R. (2018). Increasing magnitude of hurricane rapid intensification in the central and eastern tropical Atlantic. *Geophysical Research Letters*, *45*(9), 4238–4247. https://doi.org/10.1029/2018gl077597

Balistrocchi, M., & Bacchi, B. (2011). Modelling the statistical dependence of rainfall event variables through copula functions. *Hydrology and Earth System Sciences*, *15*(6), 1959–1977. https://doi.org/10.5194/hess-15-1959-2011

Balistrocchi, M., Orlandini, S., Ranzi, R., & Bacchi, B. (2017). Copula-based modeling of flood control reservoirs. *Water Resources Research*, *53*(11), 9883–9900. https://doi.org/10.1002/2017wr021345

Bhatia, K. T., Vecchi, G. A., Knutson, T. R., Murakami, H., Kossin, J., Dixon, K. W., & Whitlock, C. E. (2019). Recent increases in tropical cyclone intensification rates. *Nature Communications*, *10*(1), 635. https://doi.org/10.1038/s41467-019-08471-z

Bloemendaal, N., Haigh, I. D., de Moel, H., Muis, S., Haarsma, R. J., & Aerts, J. C. (2020). Generation of a global synthetic tropical cyclone hazard dataset using STORM. *Scientific Data*, *7*(1), 40. https://doi.org/10.1038/s41597-020-0381-2

Bracken, C., Holman, K. D., Rajagopalan, B., & Moradkhani, H. (2018). A Bayesian hierarchical approach to multivariate nonstationary hydrologic frequency analysis. *Water Resources Research*, *54*(1), 243–255. https://doi.org/10.1002/2017wr020403

Brechmann, E. C., & Schepsmeier, U. (2013). Modeling dependence with C-and D-vine copulas: The R package CDVine. *Journal of Statistical Software*, *52*(3), 1–27. https://doi.org/10.18637/jss.v052.i03

Brunner, M. I., Seibert, J., & Favre, A. C. (2016). Bivariate return periods and their importance for flood peak and volume estimation. *Wiley Interdisciplinary Reviews: Water*, *3*(6), 819–833. https://doi.org/10.1002/wat2.1173

Camelo, J., Mayo, T. L., & Gutmann, E. D. (2020). Projected climate change impacts on hurricane storm surge inundation in the coastal United States. *Frontiers in Built Environment*, *6*, 207. https://doi.org/10.3389/fbuil.2020.588049

Chebana, F., & Ouarda, T. B. (2011). Multivariate quantiles in hydrological frequency analysis. *Environmetrics*, *22*(1), 63–78. https://doi.org/10.1002/env.1027

Clayton, D. G. (1978). A model for association in bivariate life tables and its application in epidemiological studies of familial tendency in chronic disease incidence. *Biometrika*, *65*(1), 141–151. https://doi.org/10.1093/biomet/65.1.141

Coles, S., Bawa, J., Trenner, L., & Dorazio, P. (2001). *An introduction to statistical modeling of extreme values* (Vol. 208, p. 208). Springer.

Daneshkhah, A., Remesan, R., Chatrabgoun, O., & Holman, I. P. (2016). Probabilistic modeling of flood characterizations with parametric and minimum information pair-copula model. *Journal of Hydrology*, *540*, 469–487. https://doi.org/10.1016/j.jhydrol.2016.06.044

Delignette-Muller, M. L., & Dutang, C. (2015). Fitdistrplus: An R package for fitting distributions. *Journal of Statistical Software*, *64*(4), 1–34. https://doi.org/10.18637/jss.v064.i04

Dinan, T. (2017). Projected increases in hurricane damage in the United States: The role of climate change and coastal development. *Ecological Economics*, *138*, 186–198. https://doi.org/10.1016/j.ecolecon.2017.03.034

Dupuis, D. J. (2007). Using copulas in hydrology: Benefits, cautions, and issues. *Journal of Hydrologic Engineering*, *12*(4), 381–393. https://doi.org/10.1061/(asce)1084-0699(2007)12:4(381)

Eckhardt, K. (2005). How to construct recursive digital filters for baseflow separation. *Hydrological Processes: An International Journal*, *19*(2), 507–515. https://doi.org/10.1002/hyp.5675

Elsner, J. B., Jagger, T. H., & Tsonis, A. A. (2006). Estimated return periods for hurricane Katrina. *Geophysical Research Letters*, *33*(8). https://doi.org/10.1029/2005gl025452

Elsner, J. B., & Kara, A. B. (1997). Hurricane return periods along the Gulf Coast and Florida.

Emanuel, K. (2011). Global warming effects on US hurricane damage. *Weather, Climate, and Society*, *3*(4), 261–268. https://doi.org/10.1175/wcas-d-11-00007.1

Emanuel, K. (2017). Assessing the present and future probability of Hurricane Harvey's rainfall. *Proceedings of the National Academy of Sciences*, *114*(48), 12681–12684. https://doi.org/10.1073/pnas.1716222114

Emanuel, K., & Jagger, T. (2010). On estimating hurricane return periods. *Journal of Applied Meteorology and Climatology*, *49*(5), 837–844. https://doi.org/10.1175/2009jamc2236.1

Embrechts, P., Lindskog, F., & McNeil, A. (2001). Modelling dependence with copulas. *Rapport technique, Département de mathématiques, Institut Fédéral de Technologie de Zurich, Zurich*, *14*, 1–50.

Engeland, K., Hisdal, H., & Frigessi, A. (2004). Practical extreme value modelling of hydrological floods and droughts: A case study. *Extremes*, *7*(1), 5–30. https://doi.org/10.1007/s10687-004-4727-5

Estrada, F., Botzen, W. W., & Tol, R. S. (2015). Economic losses from US hurricanes consistent with an influence from climate change. *Nature Geoscience*, *8*(11), 880–884. https://doi.org/10.1038/ngeo2560

Faranda, D., Lucarini, V., Turchetti, G., & Vaienti, S. (2011). Numerical convergence of the block-maxima approach to the generalized extreme value distribution. *Journal of Statistical Physics*, *145*(5), 1156–1180. https://doi.org/10.1007/s10955-011-0234-7

Favre, A. C., El Adlouni, S., Perreault, L., Thiemonge, N., & Bobee, B. (2004). Multivariate hydrological frequency analysis using copulas. *Water Resources Research*, *40*(1). https://doi.org/10.1029/2003wr002456

FEMA (2022). *Hazus hurricane model technical manual, Hazus 5.1*. Federal Emergency Management Agency.

Ferreira, A., & De Haan, L. (2015). On the block maxima method in extreme value theory: PWM estimators. *Annals of Statistics*, *43*(1), 276–298. https://doi.org/10.1214/14-aos1280

Folli, G. S., Nascimento, M. H., de Paulo, E. H., da Cunha, P. H., Romão, W., & Filgueiras, P. R. (2020). Variable selection in support vector regression using angular search algorithm and variance inflation factor. *Journal of Chemometrics*, *34*(12), e3282. https://doi.org/10.1002/cem.3282

Frank, M. J. (1979). On the simultaneous associativity of F (x, y) and x+ y-F (x, y). *Aequationes Mathematicae*, *19*(1), 194–226. https://doi.org/10.1007/bf02189866

Genest, C., & Favre, A. C. (2007). Everything you always wanted to know about copula modeling but were afraid to ask. *Journal of Hydrologic Engineering*, *12*(4), 347–368. https://doi.org/10.1061/(asce)1084-0699(2007)12:4(347)

Genest, C., Favre, A. C., Beliveau, J., & Jacques, C. (2007). Metaelliptical copulas and their use in frequency analysis of multivariate hydrological data. *Water Resources Research*, *43*(9). https://doi.org/10.1029/2006wr005275

Goel, N. K., Kurothe, R. S., Mathur, B. S., & Vogel, R. M. (2000). A derived flood frequency distribution for correlated rainfall intensity and duration. *Journal of Hydrology*, *228*(1–2), 56–67. https://doi.org/10.1016/s0022-1694(00)00145-1

Gori, A., Lin, N., Xi, D., & Emanuel, K. (2022). Tropical cyclone climatology change greatly exacerbates US extreme rainfall–surge hazard. *Nature Climate Change*, *12*(2), 171–178. https://doi.org/10.1038/s41558-021-01272-7

Grinsted, A., Moore, J. C., & Jevrejeva, S. (2012). Homogeneous record of Atlantic hurricane surge threat since 1923. *Proceedings of the National Academy of Sciences*, *109*(48), 19601–19605. https://doi.org/10.1073/pnas.1209542109

Gumbel, E. J. (1960). *Distributions de valeurs extrêmes en plusieurs dimensions* (Vol. 9, pp. 171–173). Publications de l'Institut de Statistique de l'Université de Paris.

Guo, Y., & Baetz, B. W. (2007). Sizing of rainwater storage units for green building applications. *Journal of Hydrologic Engineering*, *12*(2), 197–205. https://doi.org/10.1061/(asce)1084-0699(2007)12:2(197)

Harr, P. A., Jordi, A., & Madaus, L. (2022). Analysis of the future change in frequency of tropical cyclone-related impacts due to compound extreme events. In *Hurricane risk in a changing climate* (pp. 87–120). Springer International Publishing.

Hassini, S., & Guo, Y. (2016). Exponentiality test procedures for large samples of rainfall event characteristics. *Journal of Hydrologic Engineering*, *21*(4), 04016003. https://doi.org/10.1061/(asce)he.1943-5584.0001352

Holland, G., & Bruyère, C. L. (2014). Recent intense hurricane response to global climate change. *Climate Dynamics*, *42*(3–4), 617–627. https://doi.org/10.1007/s00382-013-1713-0

Hosseini, S. R., Scaioni, M., & Marani, M. (2018). On the influence of global warming on Atlantic hurricane frequency. *The International Archives of the Photogrammetry, Remote Sensing and Spatial Information Sciences*, *42*(3), 527–532. https://doi.org/10.5194/isprs-archives-xlii-3-527-2018

Joe, H. (1997). *Multivariate models and multivariate dependence concepts*. CRC Press.

Joe, H. & Kurowicka, D. (Eds.) (2011). *Dependence modeling: Vine copula handbook*. World Scientific.

Jun, C., Qin, X., Tung, Y. K., & De Michele, C. (2018). Storm event-based frequency analysis method. *Hydrology Research*, *49*(3), 700–710. https://doi.org/10.2166/nh.2017.175

Kao, S. C., & Govindaraju, R. S. (2007). A bivariate frequency analysis of extreme rainfall with implications for design. *Journal of Geophysical Research*, *112*(D13). https://doi.org/10.1029/2007jd008522

Katz, R. W., Parlange, M. B., & Naveau, P. (2002). Statistics of extremes in hydrology. *Advances in Water Resources*, *25*(8–12), 1287–1304. https://doi.org/10.1016/s0309-1708(02)00056-8

Keellings, D., & Hernández Ayala, J. J. (2019). Extreme rainfall associated with Hurricane Maria over Puerto Rico and its connections to climate variability and change. *Geophysical Research Letters*, *46*(5), 2964–2973. https://doi.org/10.1029/2019gl082077

Keim, B. D., Muller, R. A., & Stone, G. W. (2007). Spatiotemporal patterns and return periods of tropical storm and hurricane strikes from Texas to Maine. *Journal of Climate*, *20*(14), 3498–3509. https://doi.org/10.1175/jcli4187.1

Knabb, R. D., Rhome, J. R., & Brown, D. P. (2023). *Tropical cyclone report: Hurricane Katrina, 23–30 August 2005*. National Hurricane Center.

Knutson, T., Camargo, S. J., Chan, J. C., Emanuel, K., Ho, C. H., Kossin, J., et al. (2020). Tropical cyclones and climate change assessment: Part II: Projected response to anthropogenic warming. *Bulletin of the American Meteorological Society*, *101*(3), E303–E322. https://doi.org/10.1175/bams-d-18-0194.1

Ko, V., & Hjort, N. L. (2019). Model robust inference with two-stage maximum likelihood estimation for copulas. *Journal of Multivariate Analysis*, *171*, 362–381. https://doi.org/10.1016/j.jmva.2019.01.004

Kossin, J. P., Knapp, K. R., Olander, T. L., & Velden, C. S. (2020). Global increase in major tropical cyclone exceedance probability over the past four decades. *Proceedings of the National Academy of Sciences*, *117*(22), 11975–11980. https://doi.org/10.1073/pnas.1920849117

Kraus, D., & Czado, C. (2017). D-vine copula based quantile regression. *Computational Statistics & Data Analysis*, *110*, 1–18. https://doi.org/10.1016/j.csda.2016.12.009

Kurothe, R. S., Goel, N. K., & Mathur, B. S. (1997). Derived flood frequency distribution for negatively correlated rainfall intensity and duration. *Water Resources Research*, *33*(9), 2103–2107. https://doi.org/10.1029/97wr00812

Kwon, H. H., & Lall, U. (2016). A copula-based nonstationary frequency analysis for the 2012–2015 drought in California. *Water Resources Research*, *52*(7), 5662–5675. https://doi.org/10.1002/2016wr018959

Laio, F., Di Baldassarre, G., & Montanari, A. (2009). Model selection techniques for the frequency analysis of hydrological extremes. *Water Resources Research*, *45*(7). https://doi.org/10.1029/2007wr006666

Latif, S., & Simonovic, S. P. (2022). Parametric Vine copula framework in the trivariate probability analysis of compound flooding events. *Water*, *14*(14), 2214. https://doi.org/10.3390/w14142214

Lee, C. H., Kim, T. W., Chung, G., Choi, M., & Yoo, C. (2010). Application of bivariate frequency analysis to the derivation of rainfall frequency curves. *Stochastic Environmental Research and Risk Assessment*, *24*(3), 389–397. https://doi.org/10.1007/s00477-009-0328-9

Li, H., Wang, D., Singh, V. P., Wang, Y., Wu, J., Wu, J., et al. (2019). Non-stationary frequency analysis of annual extreme rainfall volume and intensity using Archimedean copulas: A case study in eastern China. *Journal of Hydrology*, *571*, 114–131. https://doi.org/10.1016/j.jhydrol.2019.01.054

Li, X., Fu, D., Nielsen-Gammon, J., Gangrade, S., Kao, S. C., Chang, P., et al. (2023). Impacts of climate change on future hurricane induced rainfall and flooding in a coastal watershed: A case study on hurricane Harvey. *Journal of Hydrology*, *616*, 128774. https://doi.org/10.1016/j.jhydrol.2022.128774

Lin, N., Emanuel, K., Oppenheimer, M., & Vanmarcke, E. (2012). Physically based assessment of hurricane surge threat under climate change. *Nature Climate Change*, *2*(6), 462–467. https://doi.org/10.1038/nclimate1389

Lindsey, C., & Sheather, S. (2010). Variable selection in linear regression. *STATA Journal*, *10*(4), 650–669. https://doi.org/10.1177/1536867x1001000407

Lombardo, F., Napolitano, F., Russo, F., & Koutsoyiannis, D. (2019). On the exact distribution of correlated extremes in hydrology. *Water Resources Research*, *55*(12), 10405–10423. https://doi.org/10.1029/2019wr025547

Lu, P., Lin, N., Emanuel, K., Chavas, D., & Smith, J. (2018). Assessing hurricane rainfall mechanisms using a physics-based model: Hurricanes Isabel (2003) and Irene (2011). *Journal of the Atmospheric Sciences*, *75*(7), 2337–2358. https://doi.org/10.1175/jas-d-17-0264.1

Marsooli, R., Lin, N., Emanuel, K., & Feng, K. (2019). Climate change exacerbates hurricane flood hazards along US Atlantic and Gulf Coasts in spatially varying patterns. *Nature Communications*, *10*(1), 3785. https://doi.org/10.1038/s41467-019-11755-z

Massey, F. J., Jr. (1951). The Kolmogorov-Smirnov test for goodness of fit. *Journal of the American Statistical Association*, *46*(253), 68–78. https://doi.org/10.1080/01621459.1951.10500769

Mayo, T. L., & Lin, N. (2022). Climate change impacts to the coastal flood hazard in the northeastern United States. *Weather and Climate Extremes*, *36*, 100453. https://doi.org/10.1016/j.wace.2022.100453

McDonald, W. M., & Naughton, J. B. (2019). Impact of hurricane Harvey on the results of regional flood frequency analysis. *Journal of Flood Risk Management*, *12*(S1), e12500. https://doi.org/10.1111/jfr3.12500

Meng, C., Xu, W., Qiao, Y., Liao, X., & Qin, L. (2021). Quantitative risk assessment of population affected by tropical cyclones through joint consideration of extreme precipitation and strong wind—A case study of Hainan province. *Earth's Future*, *9*(12), e2021EF002365. https://doi.org/10.1029/2021ef002365

Ming, X., Liang, Q., Dawson, R., Xia, X., & Hou, J. (2022). A quantitative multi-hazard risk assessment framework for compound flooding considering hazard inter-dependencies and interactions. *Journal of Hydrology*, *607*, 127477. https://doi.org/10.1016/j.jhydrol.2022.127477

Muthuvel, D., & Mahesha, A. (2021). Copula-based frequency and coincidence risk analysis of floods in tropical-seasonal rivers. *Journal of Hydrologic Engineering*, *26*(5), 05021007. https://doi.org/10.1061/(asce)he.1943-5584.0002061

National Hurricane Center (NHC). (2022). Tropical cyclone report: Hurricane ian (AL092022). Retrieved from https://www.nhc.noaa.gov/data/tcr/AL092022_Ian.pdf

Needham, H. F., Keim, B. D., Sathiaraj, D., & Shafer, M. (2012). Storm surge return periods for the United States Gulf Coast. In *In World environmental and water resources congress 2012: Crossing boundaries* (pp. 2422–2463).

Nelsen, R. B. (2007). *An introduction to copulas*. Springer Science & Business Media.

Nguyen, H. H., Cho, S., Jeong, J., & Choi, M. (2021). A D-vine copula quantile regression approach for soil moisture retrieval from dual polarimetric SAR Sentinel-1 over vegetated terrains. *Remote Sensing of Environment*, *255*, 112283. https://doi.org/10.1016/j.rse.2021.112283

NOAA National Centers for Environmental Information (NCEI). (2023). *U.S. Billion-dollar weather and climate disasters*. National Centers for Environmental Information.

NOAA National Centers for Environmental Information (NOAA NCEI). (2017). Data tools: Local climatological data). Retrieved from https://www.ncdc.noaa.gov/cdo-web/datasets/LCD/locations/FIPS:12/detail

NOAA National Ocean Service (NOAA NOS). (2020). Observed water levels. Retrieved from https://www.ncdc.noaa.gov/cdo-web/datasets/LCD/locations/FIPS:12/detail

Nyaupane, N., Bhandari, S., Rahaman, M. M., Wagner, K., Kalra, A., Ahmad, S., & Gupta, R. (2018). Flood frequency analysis using generalized extreme value distribution and floodplain mapping for Hurricane Harvey in Buffalo Bayou. In *World environmental and water resources congress 2018: Watershed management, irrigation and drainage, and water resources planning and management* (pp. 364–375). American Society of Civil Engineers.

Obeysekera, J., & Salas, J. D. (2016). Frequency of recurrent extremes under nonstationarity. *Journal of Hydrologic Engineering*, *21*(5), 04016005. https://doi.org/10.1061/(asce)he.1943-5584.0001339

Pant, S., & Cha, E. J. (2019). Wind and rainfall loss assessment for residential buildings under climate-dependent hurricane scenarios. *Structure and Infrastructure Engineering*, *15*(6), 771–782. https://doi.org/10.1080/15732479.2019.1572199

Parisi, F., & Lund, R. (2008). Return periods of continental US hurricanes. *Journal of Climate*, *21*(2), 403–410. https://doi.org/10.1175/2007jcli1772.1

Park, M., Yoo, C., Kim, H., & Jun, C. (2014). Bivariate frequency analysis of annual maximum rainfall event series in Seoul, Korea. *Journal of Hydrologic Engineering*, *19*(6), 1080–1088. https://doi.org/10.1061/(asce)he.1943-5584.0000891

Perica, S., Martin, D., Pavlovic, S., Roy, I., St Laurent, M., Trypaluk, C., et al. (2013). *Precipitation-frequency Atlas of the United States. Volume 9, Version 2.0. Southeastern States; Alabama, Arkansas, Florida, Georgia, Louisiana, Mississippi*. National Oceanic and Atmospheric Administration.

Phillips, R. C., Samadi, S., Hitchcock, D. B., Meadows, M. E., & Wilson, C. A. M. E. (2022). The devil is in the tail dependence: An assessment of multivariate copula-based frameworks and dependence concepts for coastal compound flood dynamics. *Earth's Future*, *10*(9), e2022EF002705. https://doi.org/10.1029/2022ef002705

Poulin, A., Huard, D., Favre, A. C., & Pugin, S. (2007). Importance of tail dependence in bivariate frequency analysis. *Journal of Hydrologic Engineering*, *12*(4), 394–403. https://doi.org/10.1061/(asce)1084-0699(2007)12:4(394)

Prosdocimi, I., Kjeldsen, T. R., & Miller, J. D. (2015). Detection and attribution of urbanization effect on flood extremes using nonstationary flood-frequency models. *Water Resources Research*, *51*(6), 4244–4262. https://doi.org/10.1002/2015wr017065

Quinn, N., Lewis, M., Wadey, M. P., & Haigh, I. D. (2014). Assessing the temporal variability in extreme storm-tide time series for coastal flood risk assessment. *Journal of Geophysical Research: Oceans*, *119*(8), 4983–4998. https://doi.org/10.1002/2014jc010197

Rappaport, E. N. (2014). Fatalities in the United States from Atlantic tropical cyclones: New data and interpretation. *Bulletin of the American Meteorological Society*, *95*(3), 341–346. https://doi.org/10.1175/bams-d-12-00074.1

Regier, E., Naughton, J., & McDonald, W. (2022). Transposing flood risk from extreme rainfall events: A case study of hurricane Harvey. *Journal of Flood Risk Management*, *15*(2), e12778. https://doi.org/10.1111/jfr3.12778

Resio, D. T., Irish, J., & Cialone, M. (2009). A surge response function approach to coastal hazard assessment–part 1: Basic concepts. *Natural Hazards*, *51*(1), 163–182. https://doi.org/10.1007/s11069-009-9379-y

Rezapour, M., & Baldock, T. E. (2014). Classification of hurricane hazards: The importance of rainfall. *Weather and Forecasting*, *29*(6), 1319–1331. https://doi.org/10.1175/waf-d-14-00014.1

Rosenblatt, M. (1952). Remarks on a multivariate transformation. *The Annals of Mathematical Statistics*, *23*(3), 470–472. https://doi.org/10.1214/aoms/1177729394

Salvadori, G., & De Michele, C. (2004). Frequency analysis via copulas: Theoretical aspects and applications to hydrological events. *Water Resources Research*, *40*(12). https://doi.org/10.1029/2004wr003133

Salvadori, G., & De Michele, C. (2007). On the use of copulas in hydrology: Theory and practice. *Journal of Hydrologic Engineering*, *12*(4), 369–380. https://doi.org/10.1061/(asce)1084-0699(2007)12:4(369)

Salvadori, G., Durante, F., & De Michele, C. (2013). Multivariate return period calculation via survival functions. *Water Resources Research*, *49*(4), 2308–2311. https://doi.org/10.1002/wrcr.20204

Schmidt, R., & Stadtmüller, U. (2006). Non-parametric estimation of tail dependence. *Scandinavian Journal of Statistics*, *33*(2), 307–335. https://doi.org/10.1111/j.1467-9469.2005.00483.x

Sebastian, T., Lendering, K., Kothuis, B., Brand, N., Jonkman, B., van Gelder, P., et al. (2017). *Hurricane Harvey report: A fact-finding effort in the direct aftermath of hurricane Harvey in the greater Houston region*. Delft University Publishers.

Serinaldi, F. (2015). Dismissing return periods. *Stochastic Environmental Research and Risk Assessment*, *29*(4), 1179–1189. https://doi.org/10.1007/s00477-014-0916-1

Shafaei, M., Fakheri-Fard, A., Dinpashoh, Y., Mirabbasi, R., & De Michele, C. (2017). Modeling flood event characteristics using D-vine structures. *Theoretical and Applied Climatology*, *130*(3–4), 713–724. https://doi.org/10.1007/s00704-016-1911-x

Shiau, J. T. (2003). Return period of bivariate distributed extreme hydrological events. *Stochastic Environmental Research and Risk Assessment*, *17*(1–2), 42–57. https://doi.org/10.1007/s00477-003-0125-9

Shimura, T., Pringle, W. J., Mori, N., Miyashita, T., & Yoshida, K. (2022). Seamless projections of global storm surge and ocean waves under a warming climate. *Geophysical Research Letters*, *49*(6), e2021GL097427. https://doi.org/10.1029/2021gl097427

Sklar, M. (1959). *Fonctions de repartition an dimensions et leurs marges* (Vol. 8, pp. 229–231). Publications de l'Institut de statistique de l'Université de Paris.

Song, J., Duan, Y., & Klotzbach, P. J. (2020). Increasing trend in rapid intensification magnitude of tropical cyclones over the western North Pacific. *Environmental Research Letters*, *15*(8), 084043. https://doi.org/10.1088/1748-9326/ab9140

Song, J. Y., Alipour, A., Moftakhari, H. R., & Moradkhani, H. (2020). Toward a more effective hurricane hazard communication. *Environmental Research Letters*, *15*(6), 064012. https://doi.org/10.1088/1748-9326/ab875f

Stone, M. (1979). Comments on model selection criteria of Akaike and Schwarz. *Journal of the Royal Statistical Society: Series B*, *41*(2), 276–278. https://doi.org/10.1111/j.2517-6161.1979.tb01084.x

Sun, F., Fu, F., Liao, H., & Xu, D. (2020). Analysis of multivariate dependent accelerated degradation data using a random-effect general Wiener process and D-vine Copula. *Reliability Engineering & System Safety*, *204*, 107168. https://doi.org/10.1016/j.ress.2020.107168

Tabari, H. (2021). Extreme value analysis dilemma for climate change impact assessment on global flood and extreme precipitation. *Journal of Hydrology*, *593*, 125932. https://doi.org/10.1016/j.jhydrol.2020.125932

Tay, R. (2017). Correlation, variance inflation and multicollinearity in regression model. *Journal of the Eastern Asia Society for Transportation Studies*, *12*, 2006–2015.

Ting, M., Kossin, J. P., Camargo, S. J., & Li, C. (2019). Past and future hurricane intensity change along the US East Coast. *Scientific Reports*, *9*(1), 1–8. https://doi.org/10.1038/s41598-019-44252-w

Treisman, R. (2022). *Damage from hurricane ian cuts Sanibel Island off from Florida's mainland*. NPR. Retrieved from https://www.npr.org/2022/09/30/1126204141/sanibel-causeway-hurricane-ian

Trepanier, J. C., Needham, H. F., Elsner, J. B., & Jagger, T. H. (2015). Combining surge and wind risk from hurricanes using a copula model: An example from Galveston, Texas. *The Professional Geographer*, *67*(1), 52–61. https://doi.org/10.1080/00330124.2013.866437

US Environmental Protection Agency (USEPA). (1986). Methodology for analysis of detention basins for control of urban runoff quality. *U.S. Environmental Protection Agency*, *440*(5), 87–001.

US Geological Survey National Water Information System (USGS NWIS). (2016). National water information system data available on the world wide web (USGS water data for the nation). Retrieved from https://waterdata.usgs.gov/nwis/uv?referred_module=sw&state_cd=fl&format=station_list&group_key=NONE

Van Oldenborgh, G. J., Van Der Wiel, K., Sebastian, A., Singh, R., Arrighi, J., Otto, F., et al. (2017). Attribution of extreme rainfall from hurricane Harvey, August 2017. *Environmental Research Letters*, *12*(12), 124009. https://doi.org/10.1088/1748-9326/aa9ef2

Vecchi, G. A., Landsea, C., Zhang, W., Villarini, G., & Knutson, T. (2021). Changes in Atlantic major hurricane frequency since the late-19th century. *Nature Communications*, *12*(1), 4054. https://doi.org/10.1038/s41467-021-24268-5

Villarini, G., Smith, J. A., Serinaldi, F., Bales, J., Bates, P. D., & Krajewski, W. F. (2009). Flood frequency analysis for nonstationary annual peak records in an urban drainage basin. *Advances in Water Resources*, *32*(8), 1255–1266. https://doi.org/10.1016/j.advwatres.2009.05.003

Volpi, E., Fiori, A., Grimaldi, S., Lombardo, F., & Koutsoyiannis, D. (2015). One hundred years of return period: Strengths and limitations. *Water Resources Research*, *51*(10), 8570–8585. https://doi.org/10.1002/2015wr017820

Vousdoukas, M. I., Voukouvalas, E., Annunziato, A., Giardino, A., & Feyen, L. (2016). Projections of extreme storm surge levels along Europe. *Climate Dynamics*, *47*(9–10), 3171–3190. https://doi.org/10.1007/s00382-016-3019-5

Vu, T. M., & Mishra, A. K. (2019). Nonstationary frequency analysis of the recent extreme precipitation events in the United States. *Journal of Hydrology*, *575*, 999–1010. https://doi.org/10.1016/j.jhydrol.2019.05.090

Wahl, T., Jain, S., Bender, J., Meyers, S. D., & Luther, M. E. (2015). Increasing risk of compound flooding from storm surge and rainfall for major US cities. *Nature Climate Change*, *5*(12), 1093–1097. https://doi.org/10.1038/nclimate2736

Weinkle, J., Landsea, C., Collins, D., Musulin, R., Crompton, R. P., Klotzbach, P. J., & Pielke, R., Jr. (2018). Normalized hurricane damage in the continental United States 1900?2017. *Nature Sustainability*, *1*(12), 808–813. https://doi.org/10.1038/s41893-018-0165-2

Weiß, G. (2011). Copula parameter estimation by maximum-likelihood and minimum-distance estimators: A simulation study. *Computational Statistics*, *26*(1), 31–54. https://doi.org/10.1007/s00180-010-0203-7

White, H. (1982). Maximum likelihood estimation of misspecified models. *Econometrica: Journal of the Econometric Society*, *50*, 1–25. https://doi.org/10.2307/1912526

Xiao, Y., Guo, S., Liu, P., Yan, B., & Chen, L. (2009). Design flood hydrograph based on multicharacteristic synthesis index method. *Journal of Hydrologic Engineering*, *14*(12), 1359–1364. https://doi.org/10.1061/(asce)1084-0699(2009)14:12(1359)

Yan, H., & Moradkhani, H. (2015). A regional Bayesian hierarchical model for flood frequency analysis. *Stochastic Environmental Research and Risk Assessment*, *29*(3), 1019–1036. https://doi.org/10.1007/s00477-014-0975-3

Yin, J., Guo, S., He, S., Guo, J., Hong, X., & Liu, Z. (2018). A copula-based analysis of projected climate changes to bivariate flood quantiles. *Journal of Hydrology*, *566*, 23–42. https://doi.org/10.1016/j.jhydrol.2018.08.053

Yoo, C., & Cho, E. (2019). Effect of multicollinearity on the bivariate frequency analysis of annual maximum rainfall events. *Water*, *11*(5), 905. https://doi.org/10.3390/w11050905

Yoo, C., Park, C., & Jun, C. (2016). Evaluation of the concept of critical rainfall duration by bivariate frequency analysis of annual maximum independent rainfall event series in Seoul, Korea. *Journal of Hydrologic Engineering*, *21*(1), 05015016. https://doi.org/10.1061/(asce)he.1943-5584.0001259

Yue, S., & Rasmussen, P. (2002). Bivariate frequency analysis: Discussion of some useful concepts in hydrological application. *Hydrological Processes*, *16*(14), 2881–2898. https://doi.org/10.1002/hyp.1185

Zhang, B., Wang, S., Moradkhani, H., Slater, L., & Liu, J. (2022). A vine copula-based ensemble projection of precipitation intensity–duration–frequency curves at sub-daily to multi-day time scales. *Water Resources Research*, *58*(11), e2022WR032658. https://doi.org/10.1029/2022wr032658

Zhang, J., Gao, K., Li, Y., & Zhang, Q. (2022). Maximum likelihood estimation methods for copula models. *Computational Economics*, *60*(1), 99–124. https://doi.org/10.1007/s10614-021-10139-0

Zhang, L., & Singh, V. P. (2006). Bivariate flood frequency analysis using the copula method. *Journal of Hydrologic Engineering*, *11*(2), 150–164. https://doi.org/10.1061/(asce)1084-0699(2006)11:2(150)

Zhang, L., & Singh, V. P. (2007). Bivariate rainfall frequency distributions using Archimedean copulas. *Journal of Hydrology*, *332*(1–2), 93–109. https://doi.org/10.1016/j.jhydrol.2006.06.033

Zhang, Q., Gu, X., Singh, V. P., & Xiao, M. (2014). Flood frequency analysis with consideration of hydrological alterations: Changing properties, causes and implications. *Journal of Hydrology*, *519*, 803–813. https://doi.org/10.1016/j.jhydrol.2014.08.011